Textile Progress

ISSN: 0040-5167 (Print) 1754-2278 (Online) Journal homepage: http://www.tandfonline.com/loi/ttpr20

Aerogels for thermal insulation in high-performance textiles

M. Venkataraman, R. Mishra, T. M. Kotresh, J. Militky & H. Jamshaid

To cite this article: M. Venkataraman, R. Mishra, T. M. Kotresh, J. Militky & H. Jamshaid (2016) Aerogels for thermal insulation in high-performance textiles, Textile Progress, 48:2, 55-118, DOI: 10.1080/00405167.2016.1179477

To link to this article: http://dx.doi.org/10.1080/00405167.2016.1179477

Published online: 31 May 2016.

TEXTILE PROGRESS, 2016
VOL. 48, NO. 2, 55–118
http://dx.doi.org/10.1080/00405167.2016.1179477

Taylor & Francis
Taylor & Francis Group

Aerogels for thermal insulation in high-performance textiles

M. Venkataraman[a], R. Mishra[a], T. M. Kotresh[b], J. Militky[a] and H. Jamshaid[a]

[a]Department of Material Engineering, Faculty of Textile Engineering, Technical University of Liberec, Liberec, Czech Republic; [b]Defence Bioengineering and Electromedical Laboratory, Defence Research and Development Organization, Bangalore, India

ABSTRACT

For many garment applications where protection is needed against hostile environments, part of the requirement is for insulation to shield the wearer from extremes of temperature. For an insulating garment to be fully effective, it needs to allow the wearer to move freely so that they can carry out their intended activity efficiently. Traditional materials achieve their insulation by trapping air within the structure thereby not only limiting heat loss by convection but also making good use of the low thermal conductivity of air to cocoon the wearer within a comfortable environment. To achieve effective protection with conventional textiles, it is usually necessary to have a thick fibrous layer, or series of layers, to trap a sufficient quantity of air to provide the required level of insulation. Several disadvantages arise as a result. For example, thick layers of insulating textile materials reduce the ability of the wearer to move in a normal manner so that the conduct of detailed manual tasks can become very difficult; the layers lose their insulating capacity when the trapped air is lost as they are compressed; the insulating capacity falls rapidly as moisture collects within the fibrous insulator – it does not have to become sensibly wet for this to happen; just 15% moisture regain can give a dramatic reduction in insulating capacity. Not surprisingly therefore, there has been continued interest in developing insulators that might be able to overcome the disadvantages of conventional textile materials and improve the mobility of the wearer by allowing the use of only a very thin layer of extremely-high insulating performance to provide the required thermal protection. One class of materials from which suitable candidates might be drawn is aerogels; their attractiveness derives from the fact that they show the highest thermal insulation capacity of any materials developed so far. Despite sporadic high levels of interest, commercialisation has been slow. Aerogels have been found to possess their own set of disadvantages such as fragility; rigidity; dust formation during working and cumbersome, expensive, batch-wise manufacturing processes. They may well have been destined to become a product of minor interest, confined to very specialist applications where cost was of little concern. However, methods have been developed to combine aerogels and fibres in composite structures which maintain extremely high insulating capacity whilst demonstrating sufficient flexibility for use in garments. Ways have been found to prevent the

ARTICLE HISTORY
Received 29 June 2015
Accepted 5 April 2016

KEYWORDS
Aerogels; high-performance thermal and acoustic insulation; hydrophobic modification; hostile environments; clothing; apparel; footwear; high–performance garments

CONTACT R. Mishra rajesh.mishra@tul.cz

formation of powder as aerogel composite fabrics are worked. Most significant though, is the achievement, arising from a project supported by the Korean Government, of a simplified one-step production process developed with the express aim of providing a substantial reduction in the cost of aerogels. Suitably-priced aerogel is now available and this should provide fresh stimulus for research and development teams to engage in new product development work utilising aerogels in textiles and garments for thermal insulation. The mechanisms through which aerogels achieve their outstanding thermal insulating ability is unconventional, at least in terms of materials used in textiles. This issue of *Textile Progress* therefore includes detail about thermal transport in aerogels before reviewing the various forms in which aerogels can now be made, some of their applications and the research priorities that are now beginning to emerge.

1. Introduction

Aerogels are highly porous materials with extreme properties [1], and although they are considered to be a 'Material of the Twenty-First Century', it was in 1930 that Kistler invented the first process for making such a highly porous inorganic silica product [2]. Aerogels are also known as frozen smoke, solid smoke, solid air, or blue smoke [3], characterized as low-density solids with a low optical index of refraction, low thermal conductivity, low speed of sound through the material, a high surface area, and a low dielectric constant. According to IUPAC, an aerogel is defined as a gel comprising a microporous solid in which the dispersed phase is a gas [4]. Aegerter et al. [5] defined aerogels as gels in which the liquid has been replaced with air, with very moderate shrinkage of the solid network. The typical structure of an aerogel is shown in Figure 1.

Although its use has been confined to very specialist applications to date, according to market research reports issued for the period 2013−2020, the global aerogel market is

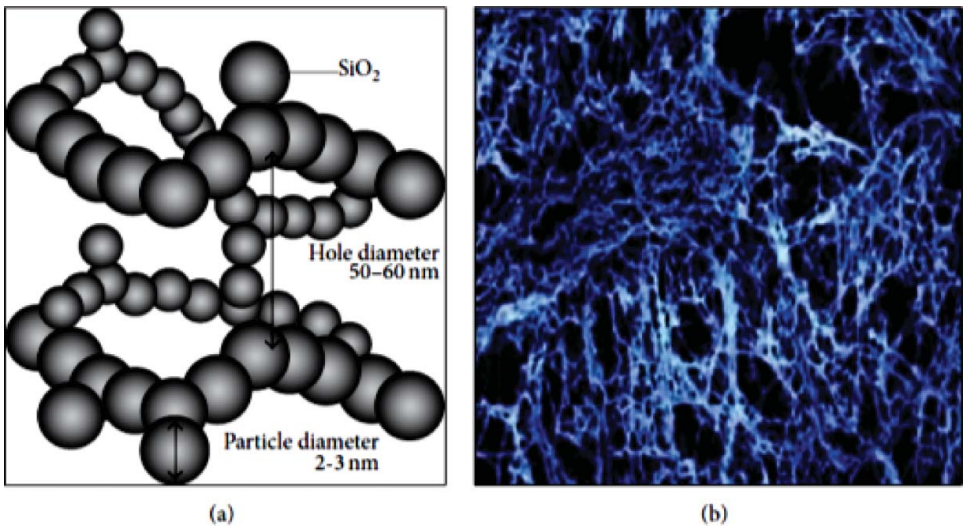

Figure 1. Nanometre scale particles and pores in an aerogel: (a) network architecture of an aerogel [143]; (b) electron micrograph of a silica aerogel [144].

forecast to reach US$1896.6 million by 2020 from $221.8 million in 2013, registering a compound annual growth rate (CAGR) of 36.4% during the forecast period (2014–2020).

North America and Europe are expected to generate about two-thirds of the market revenue by 2020. In terms of volume, the market is expected to reach 953.1 million sq. ft. of product by 2020, from 105.6 million sq. ft. in 2013. Though the consumption of aerogels is worldwide, and largely evenly dispersed, over 85% of aerogel production facilities are located in North America and Europe.

Silica, carbon, and alumina have been the prime sources for manufacturing aerogels whilst others (polymers, chalcogels, and seagels) are more scarcely used. Silica aerogel is projected to be the most promising segment, mainly due to its efficient insulation properties and the promise of lightweight solutions.

Other aerogel market segments are anticipated to grow at a CAGR of 52% during the forecast period. This includes applications in agriculture, cryogenics, apparel components, and power generation. The substantial growth of other types is mainly attributed to polymer aerogels, which are now beginning to emerge as efficient and cost-effective heat insulators.

The oil and gas sector is expected to continue to lead the global aerogel application market both in terms of value and volume through to 2020. Acoustic insulation, building insulation, and electronics applications are all also expected to show significant growth [6,7].

Aerogel materials demonstrate outstanding performance as thermal, acoustic absorbents or insulators, shock absorbers, in batteries, as electrical insulators, as catalyst supports, drug carriers, cosmic dust collectors, and in nuclear-waste storage materials [7,8]. Aerogels together with vacuum insulation panels are currently the new, promising, high-performance thermal and acoustic insulation materials for building applications [8–16]; also their high visible, solar radiation transmittance is a desirable attribute for application in insulating windows.

1.1. What is an aerogel?

An aerogel is an advanced material with an appearance of solid smoke or that of a hologram, appearing to be a projection rather than a solid object. It consists of more than 96% air. The remaining 4% is a wispy matrix of silicon dioxide. Consequently, it is one of the lowest density solids ever conceived. Aerogels are made by a 'sol–gel process', during which, in the case of silica aerogels, silicon alkoxide precursors dispersed in water undergo hydrolysis and condensation, the rates of which are controlled by the presence of a catalyst; concurrent condensation of the silicon alkoxide causes the formation of a gel network [17,18].

The mixture is a liquid at the start of the reaction, and becomes more and more viscous; as the reactions proceed, the solution loses its fluidity and the whole reaction mixture becomes a gel consisting of a three-dimensional (3D) network of silicon dioxide filled with the solvent, which in this case is water. During a specially controlled drying procedure, the solvent is extracted from the gel body without allowing the gel to collapse, leaving the intact silicon oxide network filled with air instead of water; the product is called an aerogel.

Silica aerogels (SiO_2) are highly porous, optically transparent, solid materials composed of individual particles only a few nanometres in size, which are linked in a 3D structure. Aerogels can be synthesized not only from silicon oxide (silica aerogel), but also from a variety of organic and inorganic substances such as titanium oxide, aluminium oxide, and carbon.

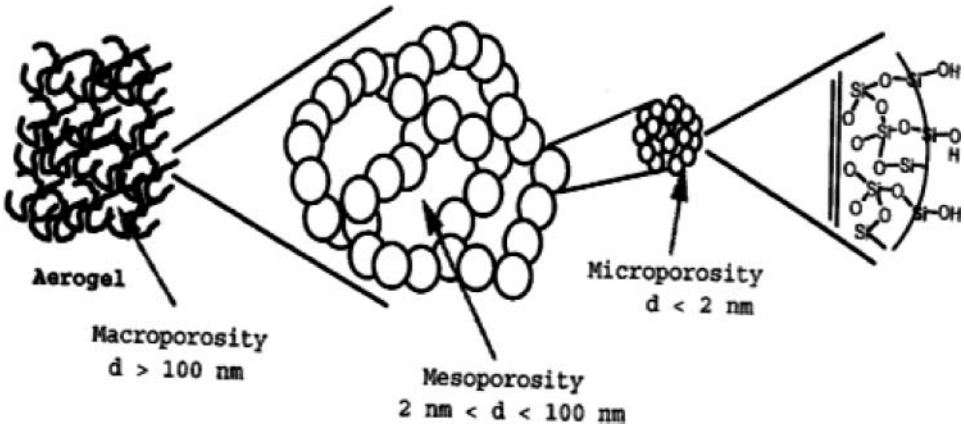

Figure 2. Complex aerogel pore structure [19].

Aerogels are distinguished by their very fine pore sizes (from about 1−20 nm) as shown in Figure 2, and can be made to have ultra-low densities. The very small pores are synonymous with very high surface areas (e.g. from 800 to 1100 m^2/g) of the internal structures.

1.2. History: the creation and evolution of aerogel

Kistler found a way to remove the fluid from a wet silica gel, leaving behind its solid structure. There is conflicting information regarding the precise timing of, and his motivation for, producing them, but throughout the 1920s, he had been working with supercritical fluids (high-pressure fluids on the point of boiling). In the early 1930s, he continued his experiments with aerogels, studying some of their thermal and catalytic properties [18]. The first commercial aerogel was produced in 1942 by the Monsanto Corporation, under the trade name Santocel. The process involved soaking a sodium silicate solution in sulphuric acid, then repeatedly washing it in alcohol before drying it at high pressure. Monsanto described the product as 'a light, friable, slightly-opalescent solid containing as much as 95 percent air by volume. It is a very-effective, heat-insulating material' [19]. Monsanto claimed to have produced an aerogel with a density of 1.8 pounds per cubic foot (29 kg/m^3), but their regular output was more dense, at between three and five pounds per cubic foot (48−80 kg/m^3). Monsanto marketed Santocel mainly as a flatting/matting agent for paints and varnishes. Its applications, though not numerous, were as varied as thermal insulation in household freezers and an ingredient in Napalm. Because of its high manufacturing cost, however, Monsanto discontinued aerogel production in 1970 [19]. Interest in aerogels, and their very low thermal conductivity, increased in the 1980s as energy conservation became more important and much of its production and applications since 1993, including some exploration of the use of aerogels in garments, have been led by Aspen, when Aspen Systems was awarded the contract by NASA for aerogel development, which was the first step leading to the launch of Aspen Aerogels Inc., Northborough, MA, in 2001 [20]. However, the high production costs of aerogels which had prevented their widespread use [20,21] continued to be an issue.

In recent years, there has been a renewed interest in aerogel research due to the changing and challenging needs of the twenty-first century and the number of patent

applications has increased dramatically. In the face of environmental change and eventual energy crisis, there is now a growing need for materials like aerogels that can conserve energy, and help to reduce greenhouse gas emissions and pollution (for instance, by use in thermal and acoustic insulation, air and water purification), but there is also recent growth in high-performance apparel applications and gloves, where aerogels' excellent insulation properties, which are retained even under compression, offer advantages when used as garment panels at particular pressure points over the usual fibrous fillings such as polyester [22]. Difficulties which might otherwise arise in cutting and sewing/joining of the aerogel in garment manufacture, can be obviated by encapsulation of the aerogel, for example, as offered in Aerotherm insulation panel sets (Aerogel Technologies Inc. Boston, MA) [23]. The same attribute of insulation retention under compression also makes aerogels an excellent choice for the creation of insulating insoles in footwear. Its use as a component of firefighters' protective clothing is also being explored [24–26].

Thermal conduction through the solid structure of an aerogel is limited by the small contact surface between the particles from which it is composed. Gaseous conduction is limited because the cells/pores are so small – around the size of the mean free path for collisions between molecules of the gases from which the air is composed. The gas molecules collide with the solid network and cannot, therefore, transfer their energy to a neighbouring gas molecule. Radiative transmission is low because silica aerogels possess low transparency to infrared (IR) radiation. Aerogels, with their extremely low thermal conductivity, derived from these physical properties are, therefore, an attractive proposition for making insulating materials, and whilst the global market for aerogel is growing rapidly, recent growth has been driven primarily by insulation applications [22] and intensive research activities have been focused on their technological development and commercial application.

The wider application of aerogels has been dogged by the high costs associated with their production; hence there is interest in improving the methods of manufacture. For example, several processes have been developed for preparing monolithic aerogel with low bulk densities, at ambient pressure without the need for any solvent exchange and surface modification [23–26]. This has been achieved through the use of specific precursors like methyltrimethoxysilane (MTMS) or a combination of MTMS and vinyltrimethoxysilane, coupled with specifically-tailored processing conditions. It is the type of precursor used that largely determines the flexibility and hydrophobic characteristics of the resultant aerogel [23–27].

1.3. Structural features

Aerogels possess an unusual combination of high porosity and small pore size, making porosity characterization by conventional techniques very difficult. Techniques such as mercury intrusion, thermoporometry, and nitrogen adsorption/desorption based on the application of capillary pressures on the aerogel network, may cause large volumetric compressions, leading to incorrect values for pore size and volume [28]. Aerogels' very low permeability can be explained in terms of its pore size being suitable for transport of water vapour/gases but not for liquid water [29].

Some aerogels such as carbon aerogels can be obtained in the form of monoliths, beads, powders, or thin films, and this variety of forms makes them promising materials for application in adsorption and catalysis [30, 31]. Organic polymer aerogels are

Table 1. Characteristics of aerogels.

(1) Property	(i) Ultra-low thermal conductivity (ii) Ultra-low refractive index (iii) Ultra-low dielectric constant (iv) High surface area (v) High refractive index (vi) Ultra-low relative density (vii) Ultra-high porosity
(2) Structure	(i) Gel-like structure on nanoscale coherent skeletons and pores (ii) Hierarchical and fractal microstructure (iii) Macroscopic monolith (iv) Randomly cross-linked network (v) Non-crystalline

nanoporous materials whose nanopore structures may be modified by the chemical reactions taking place, so carbon nanotubes are added with the organic aerogel precursor. This enables potential improvements over current carbon aerogels for applications such as sensors, actuators, electrodes, and thermoelectric devices [32].

Their porosity provides both molecular accessibility and rapid mass transport via diffusion and, for these reasons, aerogels played a role in the heterogeneous catalytic materials field for over 50 years; their high porosity and the mesoscopic pore diameters of aerogel structures enable electrolytes to penetrate the aerogel particle [33].

Aerogels' characteristics and properties are given in Tables 1 and 2.

By tailoring the production process, many of the properties of an aerogel can be adjusted. Bulk density is a good example, adjusted simply by making a more- or less-concentrated precursor gel; the thermal conductivity of aerogels can also be adjusted this way, because thermal conductivity is related to density. Typically, aerogels exhibit bulk densities ranging from 0.5 to 0.01 g/cm^3 and surface areas ranging from 100 to 1000 m^2/g, depending on the composition of the aerogel and the density of the precursor gel used to make the aerogel [34,35].

Properties such as transparency, colour, mechanical strength, and susceptibility to water, however, depend primarily on the composition of the aerogel. For example, silica aerogels are usually transparent with a characteristic blue cast due to Rayleigh scattering

Table 2. Properties of aerogel.

Property	Value	Comments
Apparent density	0.03−0.35 g/cm^3	Most common density is ∼0.1 g/cm^3
Internal surface area	600−1000 m^2/g	As determined by nitrogen adsorption/desorption
% Solids	0.13%–15%	Typically, 5% solid (95% free space)
Mean pore diameter	∼20 nm	As determined by nitrogen adsorption/desorption (varies with density)
Primary particle diameter	2−5 nm	Determined by electron microscopy
Index of refraction	1.0−1.05	Very low for a solid material
Thermal tolerance	to 500 °C	Shrinkage begins slowly at 500 °C, increases with rise in temperature. Melting point is >1200 °C.
Coefficient of thermal expansion	2.0−4.0 × 10^{-6}	Determined using ultrasonic methods
Poisson's ratio	0.2	Independent of density. Similar to dense silica.
Young's modulus	10^6-10^7 N/m^2	Very small (<10^4 x) compared to dense silica
Tensile strength	16 kPa	For density = 0.1 g/cm^3
Fracture toughness	∼0.8 kPa m$^{1/2}$	For density = 0.1 g/cm^3. Determined by three-point bending.
Dielectric constant	∼1.1	For density = 0.1 g/cm^3. Very low for a solid material.
Sound velocity through the medium	100 m/s	For density = 0.07 g/cm^3. One of the lowest velocities for a solid material.

Table 3. Guinness World Records held by aerogels.

Silica aerogel	Lowest density solid (0.0011 g/cm^3) Lowest optical index of refraction (1.002) Lowest thermal conductivity (0.016 W/m/K) Lowest speed of sound through a material (70 m/s) Lowest dielectric constant from 3−40 GHz (1.008)
Carbon aerogel	Highest specific surface area for a monolithic material (3200 m/g)

of the short wavelengths of light. Carbon aerogels, on the other hand, are opaque and black, whilst iron oxide aerogels are barely translucent and can be either rust-coloured or yellow. As another example, low-density (<0.1 g/cm^3) inorganic aerogels are both excellent thermal insulators and excellent dielectric materials (electrical insulators), whereas most carbon aerogels are thermal insulators and electrical conductors. Table 3 shows some of the world records held by particular aerogels.

1.4. Classification of aerogels

Aerogels can be classified in a variety of ways as shown in Table 4.

The term aerogel does not refer to a particular substance, but rather to a geometry into which a substance can be formed; in much the same way that a sculpture can be made out of clay, plastic, papier-mâché, aerogels can be made from a wide variety of substances as shown in Table 5.

Table 4. Classification of aerogels.

(a) On the basis of appearance	(i) Monolith (ii) Powder (iii) Film/felts
(b) On the basis of preparation method	(i) Aerogel (ii) Xerogel (iii) Cryogel (iv) Other aerogel-related materials
(c) On the basis of different microstructures	(i) Microporous aerogel (<2 nm) (ii) Mesoporous aerogel (2−50 nm) (iii) Mixed porous aerogel
(d) On the basis of chemical structure	(i) Oxides (ii) Polymers (iii) Mixed (iv) Hybrid (v) Composite.

Table 5. Substances from which aerogels have been made.

Silica	
Transition metal oxides:	Iron oxide
Lanthanide and actinide metal oxides:	Praseodymium oxide
Main group metal oxides:	Tin oxide
Organic polymers:	Resorcinol/formaldehyde resin, phenol/formaldehyde resin, polyacrylates, polystyrenes, polyurethanes, epoxy resins
Biological polymers:	Gelatin, Pectin, Agar agar
Semiconductor nanostructures:	Cadmium selenide quantum dots
Carbon:	Carbon nanotubes
Metals:	Copper, Gold

Aerogel composites, for example, aerogels reinforced with polymer coatings or aerogels embedded with magnetic nanoparticles, are also routinely prepared [35].

2. Thermal conduction mechanism through porous aerogel

The thermal conductivity (λ) of thermal insulating materials (porous bodies) is described as follows:

$$\lambda = \lambda_{gc} + \lambda_{sc} + \lambda_c + \lambda_r \tag{2.1}$$

where λ_{gc} is thermal conduction through the air, λ_{sc} is thermal conduction through the solid, λ_c is the heat transfer by convection, and λ_r is the heat transfer by radiation.

Each of these thermal conduction mechanisms is schematically shown in Figure 3.

Thermal conductivity by a gas: Thermal energy transfer through the air under a temperature gradient can be regarded as a transport of kinetic energy driven by the collision of molecules of the different gases of which the air is composed. The thermal conductivity of a gas depends on the 'mean free path' of a gas molecules (L_f) enclosed in a narrow space, the mean pore size (L_s), and the 'mean free path' of the gas molecules in free space (L_g) as follows [36]:

$$\frac{1}{L_f} = \frac{1}{L_s} + \frac{1}{L_g} \tag{2.2}$$

which can be transformed as follows:

$$L_f = \frac{L_g}{1 + \frac{L_g}{L_s}} = \frac{L_g}{1 + \mathrm{Kn}} \tag{2.3}$$

where the symbol Kn represents the so-called Knudsen number.

Thermal conductivity by the gas in a porous solid: The Knudsen effect appears if the mean free path of the gas molecules in a porous solid exceeds the pore diameter, i.e. $\mathrm{Kn} > 1$; under these conditions, a gas molecule located inside a pore will most often ballistically strike the pore wall rather than another gas molecule; hence gas thermal

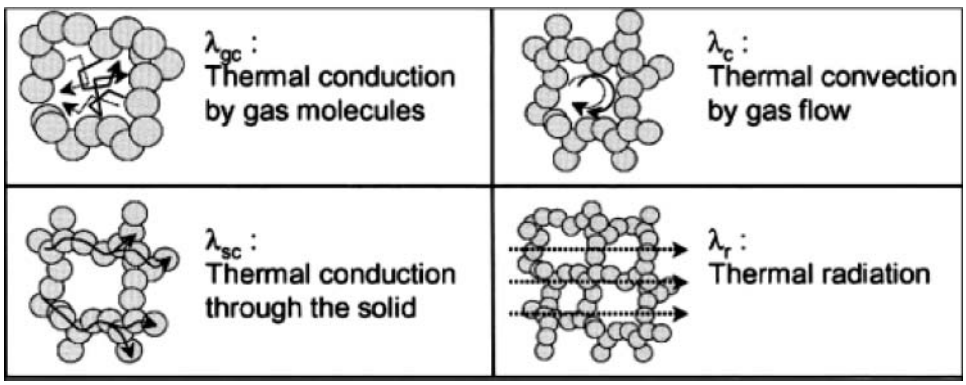

Figure 3. Factors contributing to the thermal conduction through porous materials [36].

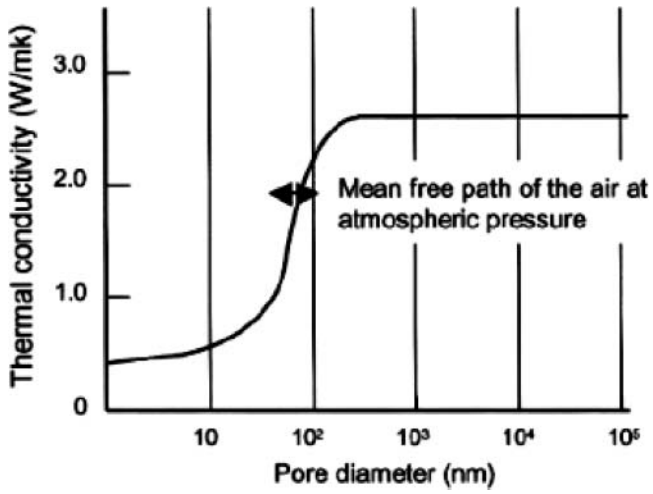

Figure 4. A rough relationship between the mean pore size (L_s) and the thermal conductivity of air [36].

conductivity, and thereby the overall thermal conductivity, becomes very low. A rough relationship between the mean pore size (L_s) and the thermal conductivity of the air is shown in Figure 4. It can be seen that, when making the mean pore size (L_s) smaller than the 'mean free path' of the gas molecules in space (L_g), L_f will be smaller and the overall thermal conduction can be less than that of the air.

Thermal conduction by the solid in a porous solid: Heat transfer by conduction involves transfer of energy within a material without any flow within the material as a whole. Thus, for a good thermal insulating material, the thermal conductivity of the material from which the solid is made should be low; it is also clear that heat transfer by thermal conductivity of a porous solid will become smaller as its structural skeleton is made thinner and the solid portion is reduced.

Convective heat transfer by the gas in a porous solid: Heat transfer by gas convection will be able to take place once the pore size becomes large enough for fluid movement to overtake molecular movement. By contrast, when the pore size is several millimetres or less, fluid movement will be suppressed and gas convection will eventually cease, even though the material remains porous.

Radiation heat transfer by a porous solid: The thermal motion of particles in a material gives rise to the emission of energy in the form of electromagnetic radiation which will transmit through the material if it is transparent to the wavelength(s) of the emitted radiation, but will be blocked if it is opaque to those wavelengths. For a porous solid, its transparency will depend on the composition of its solid component, but even so, the material as a whole will emit electromagnetic radiation to some degree given that its temperature is above 0 K or absolute zero, and more at higher temperatures. (Heat transfer by radiation from a black-body radiator increases as the fourth power of the absolute temperature and this principle needs to be taken into account for real materials in high-temperature applications [36].)

Aerogels are remarkable thermal insulators because they come close to nullifying all of these modes of heat transfer. In these materials, the mechanism of heat transfer is via lattice vibrations, as the atoms vibrating more energetically in one part of the solid transfer their thermal energy to less-energetic neighbouring atoms, an effect enhanced by

cooperative motion in the form of propagating lattice waves, which at the quantum limit are quantized as phonons [36]. The nanometre-sized pores meanwhile, partially suppress gaseous convective thermal transport and the third mode of heat transfer, radiation, comes into account only at the high temperatures. Hence, the low overall thermal conductivity of the aerogel makes it an attractive thermal insulating material.

Traditionally, for many thermal insulation applications (in ovens or heat-exchanger systems, for example), glass wool is used, but whatever the fineness of the glass wool, its sharp ends make it harmful to handle. For water coolers and refrigerators, polyurethane foam (PUF) is the usual choice of thermal insulating material. At the right price, aerogels could be used in these applications instead of glass wool or PUF, and low-cost aerogels could find applications in thermal insulating layers of clothing for very cold climates and also as water cylinder jackets. Such potential is beginning to emerge; TiO_2-doped silica aerogels prepared using low-cost sodium silicate with a reduced processing period are more economical than TiO_2-doped aerogels based on the more expensive tetraethyl orthosilicate (TEOS) precursor making them more suitable for thermal insulation in refrigerators, heat furnaces, or ovens replacing PUF and glass wool, respectively. The fine powder of superhydrophobic silica aerogel forms liquid marbles which can be used for transport of microfluids [36].

2.1. Thermal transport in monolithic aerogel

All thermal applications of silica aerogel require precise determination of their heat transfer characteristics via IR radiation and solid conduction. SiO_2 aerogel in layers of $1-2$ cm are not optically thick and, therefore, heat transfer is a complex phenomenon in this material [37].

2.1.1. Radiative heat transfer

Infrared (IR) extinction is provided by absorption. The absorption of IR radiation by aerogels is strong above IR wavelengths of 7 μm, but especially low between 3 and 5 μm as illustrated by Figure 5. Therefore, at temperatures around 280 K, the thermal IR transmission

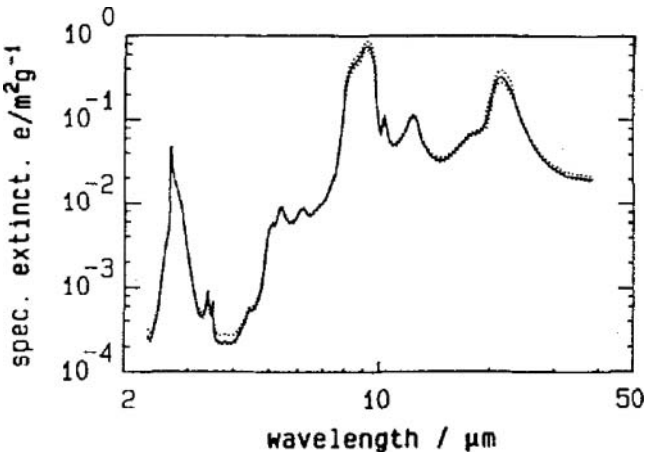

Figure 5. Specific extinction coefficient $e = E/\rho$ [37].

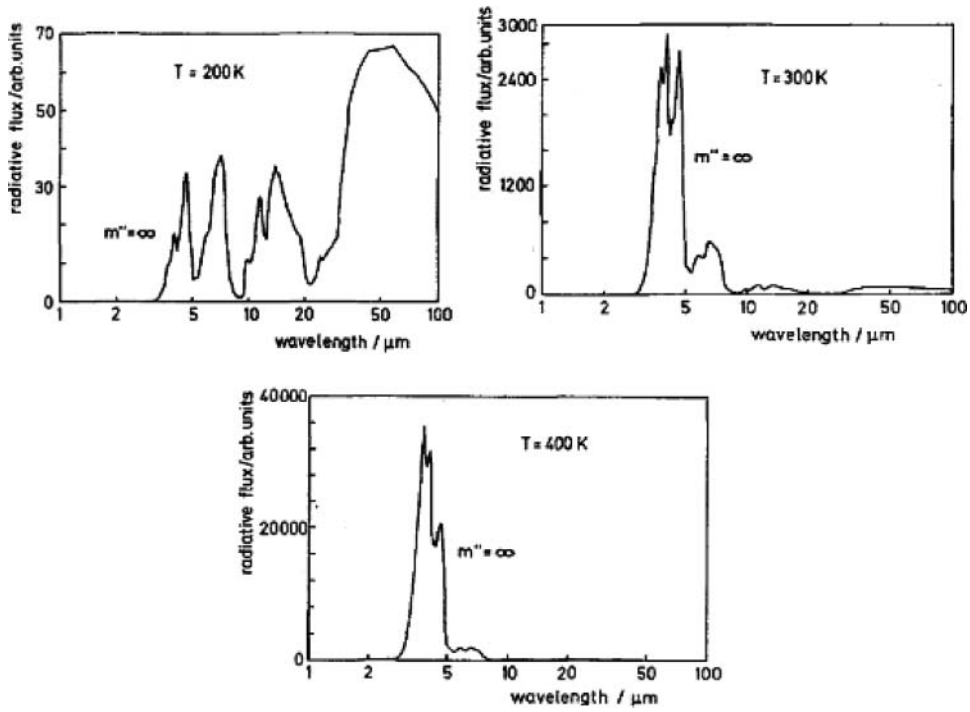

Figure 6. Relative spectral flux through silica aerogel between black boundaries for $T = 200$, 300, and 400 K [37]. (It should be noted that in Figure 6, markedly different ordinate scales are used in the charts for each different temperature.)

spectrum is effectively attenuated, and the radiative transport through aerogel is weak. For increasing temperatures, however, more and more radiation can penetrate the material within the wavelength range 3−5 μm (Figure 5). Silica aerogel then gradually loses its insulating properties [37].

In Figure 5, the specific extinction coefficient for silica aerogel at different wavelengths is shown on a logarithmic scale; the strong absorption bands shown by the silica aerogel at 9.5, 12.5 and 21 μm are also observed for silica glass; the 2.7-μm absorption band is caused by vibrations of the OH groups bound to silicon atoms in the silica [37].

For $T = 200$ K (−73 °C), the major radiative contribution occurs above wavelengths of 50 μm; low boundaries would cut off the flux maxima [37]. The tenuous structure is expected to provide a drastically reduced solid conductivity compared to silica glass. From the phonon diffusion model for non-porous SiO_2 glass (index G) and for aerogel (index A),

$$\lambda_G = C_{v,G} \cdot r_G \cdot V_G / \ 3 \tag{2.4}$$

$$\lambda_A = C_{v,A} . r_A . V_A / \ 3 \tag{2.5}$$

where λ is the thermal conductivity, C_v is the specific heat at constant volume, r is the thickness, and V is the volume; subscripts G and A refer to non-porous silica glass and aerogel, respectively.

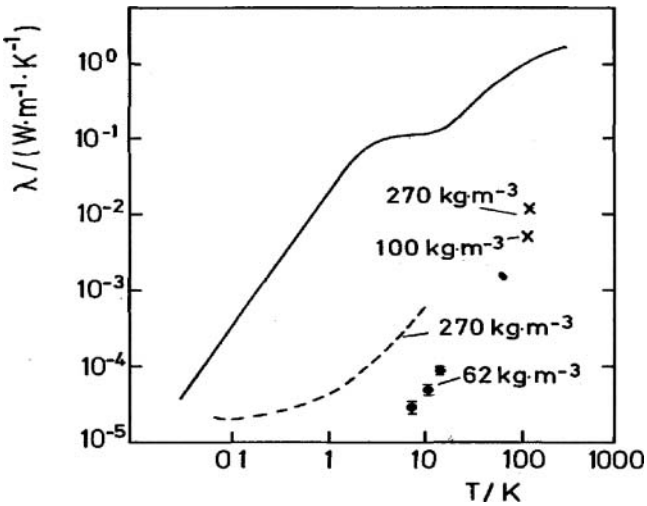

Figure 7. Double-log plot of thermal conductivity versus temperature for non-porous silica glass and aerogel having density $\rho = 270$ kg/m^3, for aerogels having densities of 100 and 62 kg/m^3, respectively [37].

The following equation has been derived as

$$\lambda_A = \lambda_G \frac{\rho_A}{\rho_G} \frac{V_A}{V_G} \tag{2.6}$$

where ρ is the density, and the subscripts G and A refer to non-porous silica glass and aerogel, respectively.

The phonon mean free paths l_p in SiO_2 glass and in silica aerogel are expected to be of the order of 1 nm. The specific heat capacities C for both materials differ markedly below 10 K; at elevated temperatures, the C_v values for glass and aerogel are comparable. For an estimate, consider aerogel with density $\rho_A = 100$ kg/m^3 and equate the phonon group velocity with the sound velocity $v_a = 100$ m/s derived from ultrasonic measurements. For $T = 300$ K (27 °C), where $\lambda_G = 1.3$ W/(m K), the value was $\lambda_A = 1.3$ W/(m K) for sound velocity (100−2200 m/s). The outcome for (100−5000 m/s) $= 10^{-3}$ W/(m K), gives a value which is by far the lowest ever reported for a solid material; the phonon diffusion model is valid at room temperature for compressed powders over a large density range. Recent measurements on the solid thermal conductivity of aerogel are presented in Figure 7. Data have been collected from stationary measurements with two 'hotplate' systems, one cooled with liquid N_2, the other with liquid He [37].

The solid thermal conductivity dramatically varies with density and the values for various densities differ (by a factor of 500 or so for the 100 kg/m^3 aerogel) between room temperature and about 4 K [37].

2.1.2. Combined radiative and conductive heat transfer

For optically thick insulations, for example, opacified fibre or powder systems, the solid and the radiative conductivities, λ_{sc} and λ_r, respectively, are well defined and are linearly

superposed:

$$\lambda = \lambda_{sc} + \lambda_r \tag{2.7}$$

with

$$\lambda_r = (16\ n^2\ \sigma\ T_r^3)\ \ (\ 3\ L\ ) \tag{2.8}$$

$$T_r = \sqrt[3]{(T_1^2 + T_2^2)\ (T_1 + T_2)} \tag{2.9}$$

$$e = L/\rho \tag{2.10}$$

where e is the specific extinction coefficient, L is the wavelength of radiative heat transfer. And ρ is the mass density. σ in Equation (2.8) is the Stefan–Boltzmann constant, n is the average index of refraction of the insulation, T_r is the mean temperature, and T_1 and T_2 in Equation (2.9) are the boundary temperatures. As λ_{sc} is only weakly dependent on temperature, the equations may be displayed in a simplified λ versus T_r^3 diagram (see Figure 8).

For optically thin, non-conducting, grey insulations with optical thickness $\tau_o = L\ d$, the radiative flux can be estimated from

$$q_r = \frac{(n^2\ \sigma\ (T_1^4 - T_2^4))}{(2/\varepsilon - 1\ + 3/4\ \tau_o)} \tag{2.11}$$

This equation will give wrong results in the general case of non-zero solid conduction and low boundary emissivities ($\varepsilon << 1$), when a considerable amount of radiation emerges from the radiative boundary layers close to the wall (Figure 9) [37].

Due to the strong temperature gradient near the wall, the energy can effectively be delivered into the boundary layers via solid conduction. The amount of radiation emitted from the boundary layers depends on its optical absorption thickness, τ_o. Furthermore,

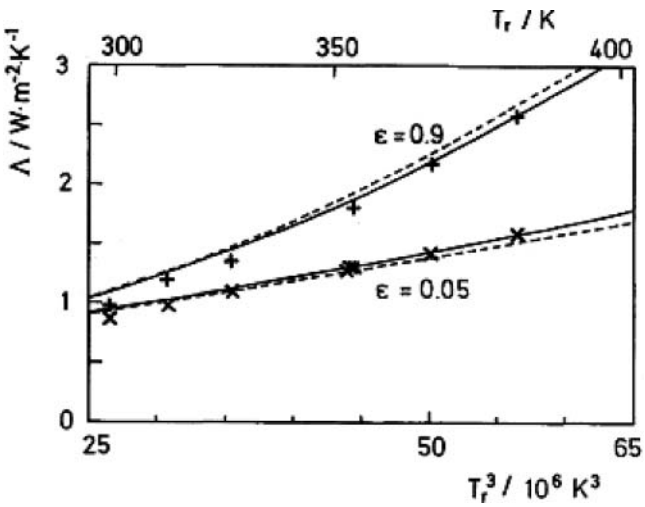

Figure 8. Thermal conductivity for an especially thick insulation; the data are for load-bearing fibre insulation [37].

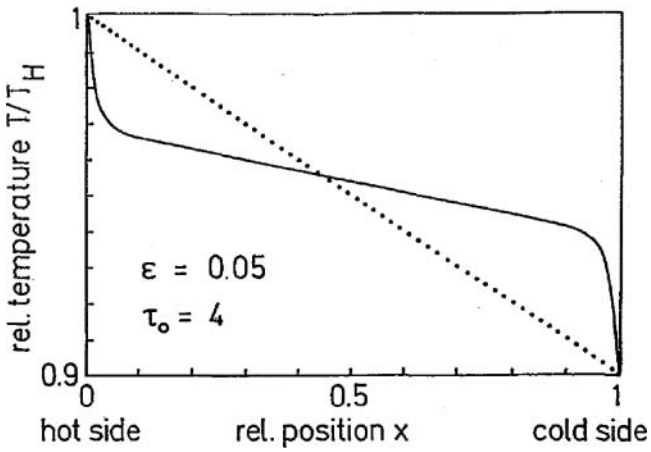

Figure 9. Temperature profile for pure conduction (dotted line) and for a medium with a radiative boundary layer (full line) [37].

the lower the emissivity (ε) of the walls for a given $\tau_{o,}$ the more radiation, compared to the emission of the walls, will proceed from the boundary layers into the aerogel tile. To take care of the boundary-layer effect, the emissivity ε in Equation (2.10) may be substituted by a (higher) effective emissivity:

$$\varepsilon' = 1 - (1 - \varepsilon) \cdot \exp\left[-\arctan(\tau_o)/2\right] \tag{2.12}$$

In general, the combined radiative and conductive heat transfer is described by an integrodifferential equation. It is tedious to solve the exact equation numerically for a non-grey medium such as aerogel, where the optical thickness τ_o is a function of wavelength. However, it is possible to work with a generalized three-flux equation, presented for grey media (see Figure 10) [37].

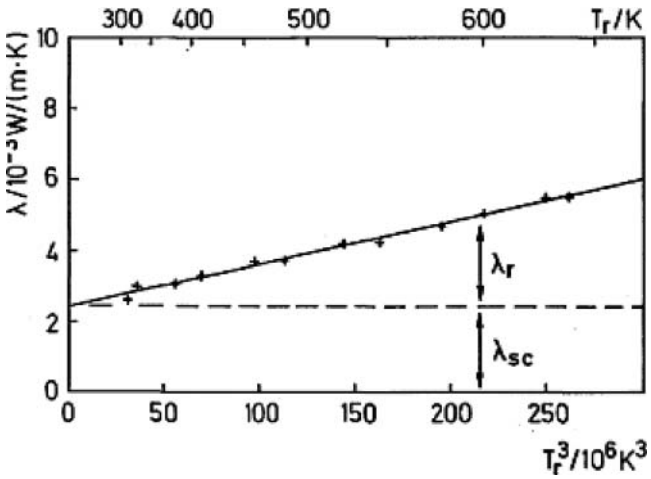

Figure 10. Thermal transfer coefficient for aerogel [37].

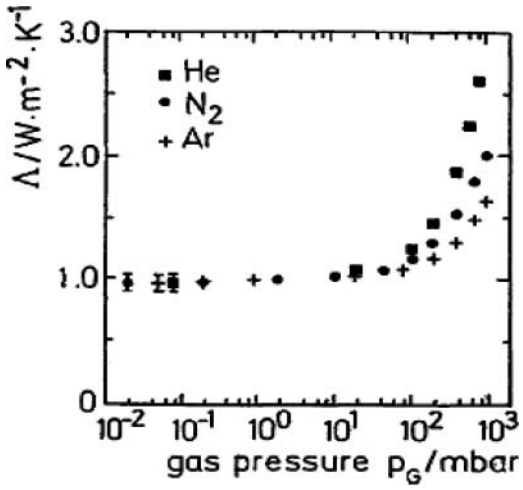

Figure 11. Thermal transfer coefficient for an 80-kg/m^3 aerogel tile of 9 mm thickness versus gas pressure; the mean temperature was $T_r = 300$ K [37].

The graphs show how the thermal transfer coefficient of an aerogel with ($\rho = 77$ kg/m^3, $d = 9$ mm) changes as a function of mean temperature T_r, where the points marked (+) are actual measurements, and the line marked (−) follows the numerical solution of the general heat transfer equation given by the approximate spectral three-flux equation [37].

2.1.3. Influence of gas pressure

The structural build-up in aerogel as determined by light scattering, SAXS, SANS, and BET measurements occurs in the 1−100 nm range. Therefore, gaseous conduction is not expected to be fully developed in aerogels, even at pressures of 1 bar. Recent measurements show that for an aerogel with a density of 80 kg/m^3, the gas-induced rise in thermal losses only occurs for pressures above 50 mbar (see Figure 11). The derived average size for the 'pores' was about 100 nm.

2.2. Thermal transport in granular aerogel

The passage of thermal energy through an insulating material occurs through three mechanisms: solid conductivity, gaseous conductivity, and radiative (IR) transmission.

The sum of these three components gives the total thermal conductivity of the material.

Fricke et al. [37] observed that both the solid conductivity and the gas conductivity were proportional to the density as follows:

$$\lambda_{gas} \alpha \rho^{-0.6} \tag{2.13}$$

$$\lambda_{solid} \alpha \rho^{1.5} \tag{2.14}$$

Hummer et al. [38] using these relations derived the following relation for radiative conductivity, which is a relative equation for the thermal conductivity of opacified silica

aerogel:

$$\lambda_{\text{total}}(\rho) = \lambda_{\text{solid},0}\left(\frac{\rho}{\rho_o}\right)^{1.5} + \lambda_{\text{gas},0}\left(\frac{\rho}{\rho_o}\right)^{-0.6} + \lambda_{\text{rad},0}\left(\frac{\rho}{\rho_o}\right)^{-1}\left(\frac{T}{T_o}\right)^{3} \tag{2.15}$$

where ρ (kg/m^3) is the density; λ_{total}, λ_{gas}, λ_{solid}, and λ_{rad} (W/m K) are the total conductivity, the conductivity for gas conduction, the conductivity for solid conduction, and the radiative conductivity, respectively; T (K) is the temperature, and the index 0 means that parameters are related to a reference material composed of pure aerogel alone.

Solid conductivity is an intrinsic property of a specific material; hence it can be reduced by appropriate selection of a different material from which to make the aerogel. A further decrease in thermal conductivity of aerogel can be achieved if it is evacuated below 50 hPa; its thermal conductivity is decreased because of elimination of the pore-filling gas which would otherwise assist in transporting at least some thermal energy through the aerogel. Super-insulation can then be achieved with evacuated highly porous powder, fibre, or gel spacers, but due to the Knudsen effect (see Equation (2.3)), even when the gas is present within an aerogel, at sufficiently small pore sizes, its thermal conductivity can be lower than that for still air, that is, even less than 25 mW/m K [38,39].

The final mode of thermal transport through silica aerogel involves infrared radiation.

2.2.1. Radiative heat transfer

IR scattering in granular fills can be neglected because of very small dimensions of pores as compared to the wavelength of light. The specific extinction coefficients resulting from absorption are expected to be comparable to those of monolithic specimens [37].

2.2.2. Solid conduction

The thermal resistance of the many contact points in granular and powderous fills can be treated according to the Kaganer model. The resulting solid conductivity is

$$\lambda_{\text{sc}} = \lambda_s \sqrt[3]{(12/\pi^2)\ (1-\mu_s^2)\ (1-\pi)^2\ \exp\ (4.8.\ (1-\pi))\ P_{\text{cxt}}/Y_s} \tag{2.16}$$

where λ_{sc} is porous solid conductivity, λ_s is the conductivity of monolith, μ_s is Poisson's ratio, P_{cxt} is the external pressure, and Y_s is Young's modulus.

For a fill in which $\rho_s = 230$ kg/m^3, $\pi = 0.34$, $Y_s = 10^7$ N/m^2, $\mu_s = 0.2$, and $P_{\text{cxt}} = 10^5$ N/m^2, which would be typical of a porous silica aerogel layer, the result is $\lambda_{\text{sc}} \approx 0.5\ \lambda_s$.

In general, one thus expects loaded (1 bar) granular fills to have half the solid conduction of monolithic layers as explained above [37].

2.2.3. Measurements on evacuated granular fills

Thermal conductivity measurements on evacuated granular aerogel layers have been performed over a temperature range from 0 to 350 °C. The tested specimen consisted of sifted pellets with diameters between 1 and 2 mm. The boundary emissivity was $\varepsilon = 0.04$

and the external load $P_{cxt} = 0.1$ bar. Surprisingly, the thermal transfer coefficient Λ showed a linear relationship when plotted against T_r^3 (i.e. the third power of the mean temperature T_r). This could falsely be interpreted as resulting from a temperature-independent extinction coefficient in an optically thick specimen. The proper interpretation, however, is that, in aerogels, the extinction coefficient markedly decreases with the rising temperature. This has two consequences:

(1) The radiative boundary-layer effect, discussed above, gets weaker with the increasing temperature.
(2) Radiation emerging from the boundary layer is attenuated less at higher temperatures.

Together, the two effects just happen to produce the result of Figure 12. In addition, it is helpful to compare the measured thermal transfer coefficient with the case of an evacuated empty spacing. The straight line in Figure 12 calculated for $\varepsilon = 0.04$ shows that thermal transport in this case is weaker, indicating that the aerogel layer roughly doubles the heat transfer [37].

The results shown were reported for an evacuated 24-mm-thick granular aerogel layer with an external load $P_{cxt} = 0.1$ bar; the boundary emissivity was $\varepsilon = 0.04$; the mass per unit area was 3.18 kg/m^2. For comparison, the transfer coefficient for an evacuated spacing had $\tau_o = 0$ [37–40]. The dependence of the thermal transfer coefficient on external load is shown in Figure 13. While below $P_{cxt} \approx 0.2$ bar, the rise is quite steep, the increase at higher loads is remarkably weak. The qualitative interpretation is that the steep rise in the early stages is caused by an increase in solid conduction combined with an enhancement of the radiative boundary layer [40–43].

Figure 13 shows results for an evacuated granular aerogel layer with the same mass per unit area as that in Figure 12; the average temperature is $T_r = 318$ K; the fit was performed

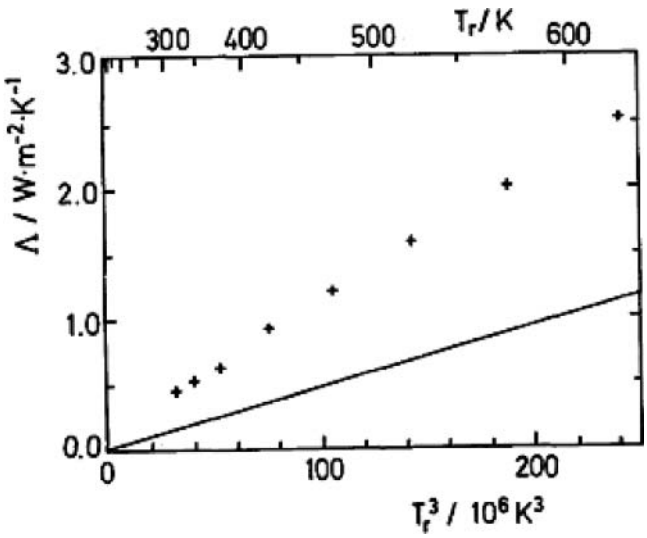

Figure 12. The thermal transfer coefficient Λ versus T_r (+++) and versus T_r^3 (straight, solid line) [37], where Λ is the thermal transfer coefficient and T_r is the mean temperature.

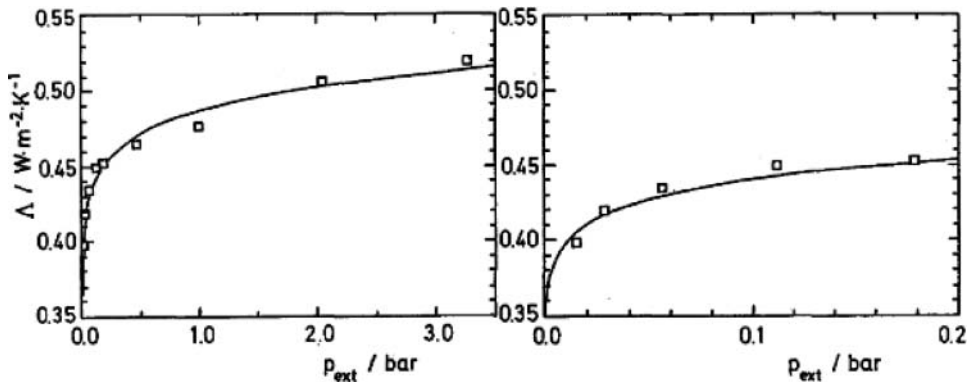

Figure 13. Thermal transfer coefficient Λ versus p_{ext} [37].

according to the following relation [37]:

$$\Lambda = \Lambda_o + \text{constant} \times (P_{ext})^{\beta}$$

where $\Lambda_o = 0.15$ W/m/K, constant $= 0.34$ W/m^2/K, P_{ext} is the external pressure $= 0.2$ bar, coefficient, $\beta \approx 1/15$.

2.2.4. Effects of gas pressure

The gas-pressure dependence of the apparent thermal conductivity shown in Figure 14 displays the two-step behaviour expected for porous materials with two distinctly different pore sizes. The fit curve represents the behaviour expected from:

$$\lambda\ (P_{GAS}) = \lambda_o + \frac{\lambda_1}{(1 + P_1/P_{GAS})} + \frac{\lambda_2}{(1 + P_2/P_{GAS})} \tag{2.17}$$

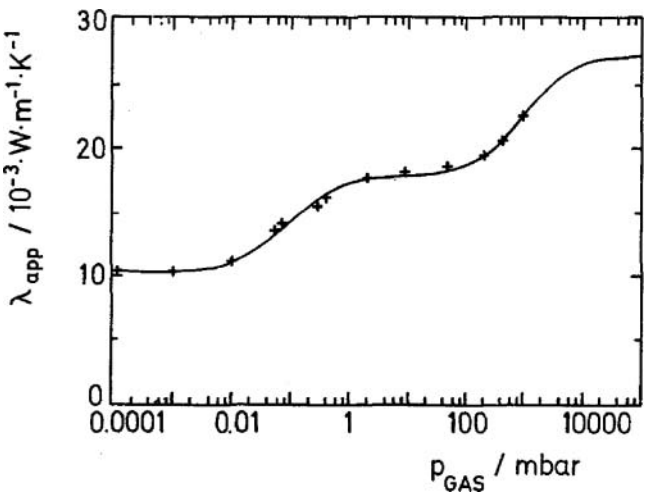

Figure 14. Measurements and fit curve for apparent total thermal conductivity, (λ_{app}), versus gas pressure (P_{GAS}), for the same granular fill as in Figure 12 at a the mean temperature of $T_r = 318$ K [37].

where $\lambda_o = 10.3 \times 10^{-3}$ W/(m K) is the conductivity for an evacuated fill, $\lambda_1 = 7.6 \times 10^{-3}$ W/(m K) represents the low pressure increase in conductivity caused by the space between the pellets, and $\lambda_2 = 9.5 \times 10^{-3}$ W/(m K) is the high pressure increase of λ caused by the pores within the pellets. $P_1 \approx 0.09$ mbar and $P_2 \approx 1050$ mbar are the pressures where $\lambda_2/2$ and $\lambda_2/2$, respectively, are reached [37].

2.2.5. Measurement of thermal conductivity of granular aerogels

Under atmospheric pressure, optimized granular aerogels show a hemispherical transmissivity of approximately 90% for a 10-mm layer [44,45]. The thermal conductivity under atmospheric pressure was measured to be approximately 22 mW/mK. Thermal stability was found using thermal gravimetric analysis for temperatures >250 °C. The thermal conductivity is influenced by the ambient pressure. Transparent granular aerogel is, therefore, not a super-insulation material, but the conductivity is remarkably reduced at pressures of approximately 50 mbar with the best results shown being 15 mW/mK at 20 °C. The influence of pressure is more important for the microstructured opaque insulation materials used for the insulation at the back of solar collector panels; for example, fumed silica reduces their thermal conductivity from 20 mW/m K at 1.000 mbar to 5 mW/m K at 10 mbar. To simulate collector working conditions, a series of measurements in evacuated systems with different pressures on the aerogel particles were performed. These tests indicated that the pressure had a low influence on thermal and optical properties. In another series of tests examining the influence of temperature and filling gases on the thermal conductivity, the increase of thermal conductivity at higher absorber temperatures was considered to be tolerable [45].

2.3. Development of silica aerogel blanket

Production of aerogels has remained a costly affair mainly due to high prices of the materials used in the production process and the relatively low production volumes. This is partly because the production process is not continuous; first, the precursor materials such as alkoxysilanes are mixed with water in a solvent. After alkoxysilane hydrolysis, a catalyst is added to start the condensation reaction to begin to yield a linked silica network in the form of a wet gel. The gel is then aged in order to strengthen the silica lattice work and hydrophobicity-imparting agents are added during the ageing process. The final step is to dry the 'wet gel' by carefully removing the liquid phase so that only the silica structure remains and does not collapse. Not surprisingly, developments in silica aerogel production today are directed towards cheaper production; there has been research interest, for example, in the use of chemical additives to reduce shrinkage during drying of the gel and enable its achievement under atmospheric conditions [46–49].

Traditionally, however, silica aerogel synthesis involves the following three steps [50]:

Step 1: Gel Preparation

The gel is prepared by the hydrolysis of silicon alkoxide precursors, such as tetramethyl orthosilicate, TEOS, methyltriethoxysilane (MTES) or a pre-polymer such as polyethoxydisiloxane in the presence of a catalyst. Concurrent condensation of the silicon alkoxide causes the formation of a gel network [51].

Step 2: Ageing

The gel is then aged in a solvent for lengthy periods of time to improve the mechanical and permeability properties of the gel network; the concentration, ageing time, temperature, pH, and polarity have a strong influence on the strength and porosity of the resultant aerogel. In laboratory settings, the batch process adopted for the ageing step is inherently a slow process. In full-scale production settings, batch processing increases product cost due to process line downtime and frequent stopping/starting of the production line; a continuous process is more desirable. However, as with any multistep process, an individual step only delays the overall process if it is allowed to become a bottleneck. Since ageing is not a heavily capital-intensive part of the process, larger ageing vessels can be used to reduce its effect on process time.

Step 3: Drying

Following ageing, the liquid inside the gel network is removed by a liquid-to-gas phase-change process. One of the problems which then arises is the need to avoid impairing or collapsing the porous texture during solvent removal, because during the solvent's evaporation intense forces from its surface tension act on the multitude of pores in the drying gel structure. In order to avoid gel collapse being brought about by these forces of surface tension, extraction of the solvent is carried out under supercritical conditions. The effects of surface tension are almost completely removed at the supercritical fluid state, as there is no distinct liquid-vapour phase boundary, so the gel structure undergoes very little internal stress whilst the solvent is being extracted. This allows the liquid to be slowly removed from the gel without causing the solid matrix in the gel to collapse from capillary action, as would happen with conventional evaporation [52,53]. High pressures are always required to achieve supercriticality, and whilst alcohols such as ethanol can be used as the solvent, supercritical CO_2 is preferred for safety reasons.

The as-produced aerogel is fragile and unsuitable for use in many practical applications unless reinforced with supports such as glass fibre, mineral fibre, or carbon fibre or cross-linked with polymers [48]. Although such reinforcement processes provide mechanical strength and flexibility to the aerogel, they may result in an undesirable increase in the thermal conductivity and density of the resulting aerogel composite, but if the mechanical requirements being placed on the aerogel by a particular application permit, the increase in thermal conductivity can be minimized by using lower volume-fractions of the (higher thermal conductivity) reinforcing fibres. The opacity of the aerogel to IR radiation may also require attention; IR opacifiers such as carbon black, titanium oxide, and iron oxide of suitable particle size may also be added during the sol−gel process to reduce the radiative component of its thermal conductivity [51]. The radiative contribution can be further reduced by incorporating IR-opacified fibres, such as PET fibres coated with carbon black.

Aspen Aerogel, Inc. uses CO_2 to dry the gels at supercritical pressure and temperature. The end result of this process is a dry, hydrophobic, nanoporous solid structure with a density around 0.1 g/cc but with a structure so delicate that it could not be practically used in its monolithic form in apparel applications. (Typical silica aerogels have an amorphous nonporous structure with about 80%−99.8% of air nanopores, high surface area (500−1200 m^2/g), low density (0.003−0.35 g/cm^3), and low thermal conductivity (0.015 W/m K) [52]). So, in order to provide a product with high durability, the aerogel is infiltrated into fibrous substrates, usually non-woven textile blankets, resulting in a flexible, drapeable aerogel

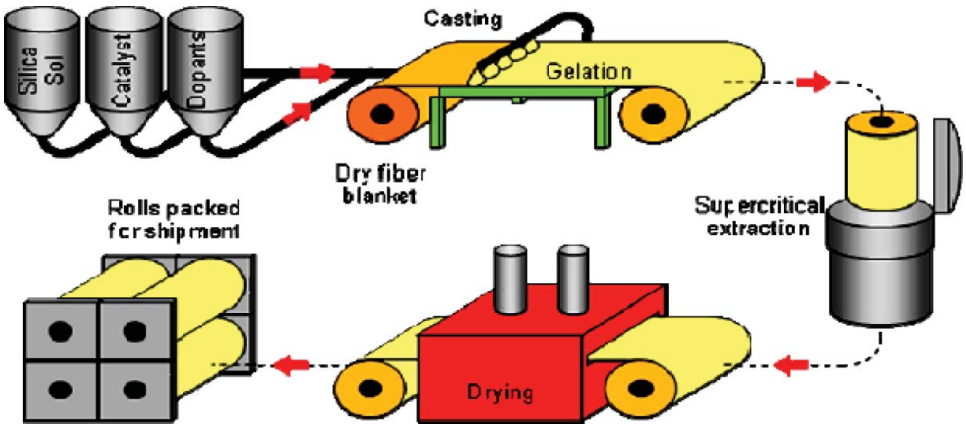

Figure 15. Production procedure for aerogel blanket [34].

composite. This product, an 'aerogel blanket', was first developed in 1999 by Aspen Systems; it finds use as insulation in aerospace applications and in industrial facilities, thanks to its low thermal conductivity and flexibility and because of the wide range of applicable temperatures under which it will operate as a high-performance insulator.

The production procedure for aerogel blanket is shown in Figure 15.

Laboratory testing has verified that insulation improvements with panels made from this type of aerogel-infiltrated blanket can approach 2.5−3 times greater than the insulation of a comparable thickness of 3M^{TM} 400 G Thinsulate^{TM} (3M, St, Paul, MN) − a popular

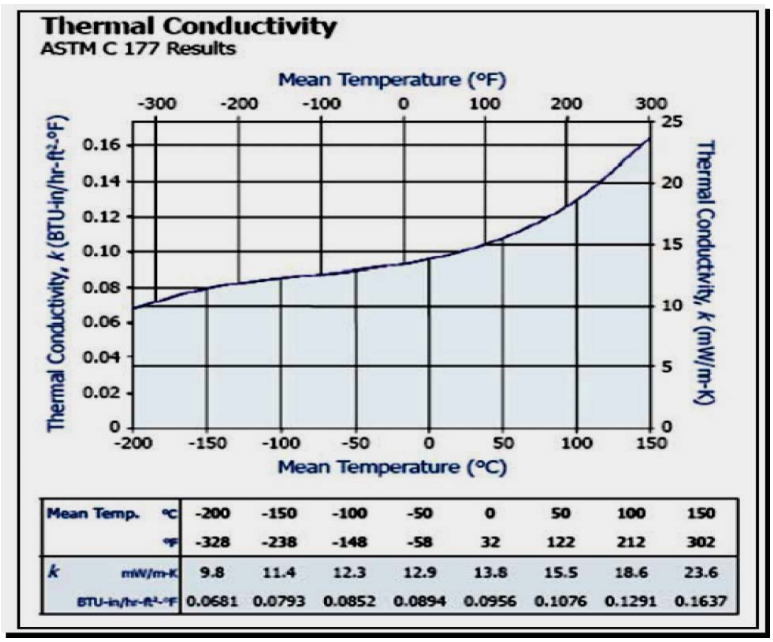

Figure 16. Thermal conductivity of aerogel at different temperatures [57].

material selection for cold-weather apparel – and over five times greater than the neoprene foam used in wetsuits. Its integration into the design of a thermal undergarment for a diver's dry suit have been shown to provide an effective thermal advantage, approximately 76% greater than a garment fabricated with a comparable thickness of 3M™ 400 G Thinsulate™ [54].

2.3.1. Thermal properties of PET/silica aerogel blanket

Aerogel blankets have proven to be effective insulators in building applications, providing the highest *R*-value of any insulation material for maximum energy efficiency in walls, floors, roofs, framing, and windows. Because flexible nanoporous PET/silica aerogel blankets possess extremely low thermal conductivity, flexibility, compression resistance, hydrophobicity, and ease of use, and given the reduced thickness and profile, it is able to provide thermal resistance at a fraction of the usual thickness of more conventional insulation. When used as insulation for buildings, therefore, it can reduce energy loss while conserving interior space in residential and commercial building applications. In some cases, thermal performance can be five times higher than other non-aerogel-based insulation materials. Blankets like Spaceloft® recover their thermal performance even after compression events as high as 50 psi [55]. The blanket combines a silica aerogel with reinforcing fibres to deliver excellent thermal performance.

The thermal conductivity of aerogel blanket is 0.011–0.015 W/m K, which is half of that of polyurethane and air [56], and the range of applicable temperatures is from −200 to 650 °C, so it has the ability to help to maintain either extremely cold or extremely hot environments. Figure 16 shows the thermal conductivity of aerogel at different temperatures. Aerogel has the flexibility and high strength to allow easy installation such as beneath underfloor heating. The density of aerogel blanket is 0.10–0.17 g/cm^3 [57]. Figure 17 shows the thermal conductivities of various insulations and Figure 18 shows the applicable temperature ranges of various insulations.

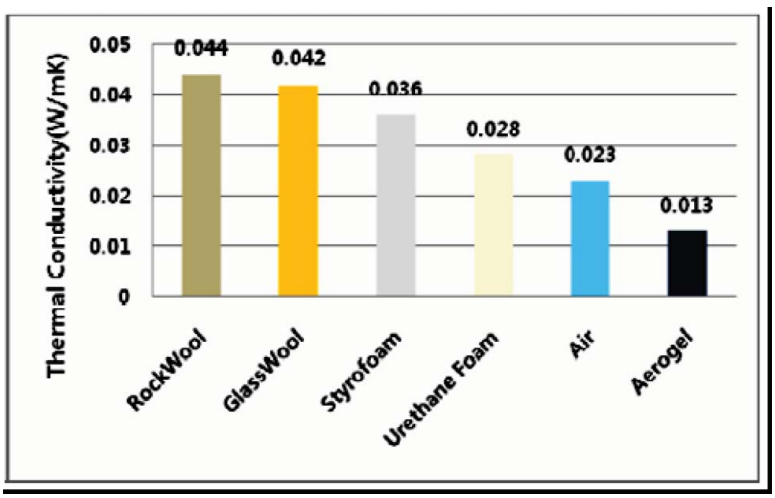

Figure 17. Thermal conductivity of a range of insulation used in buildings [57].

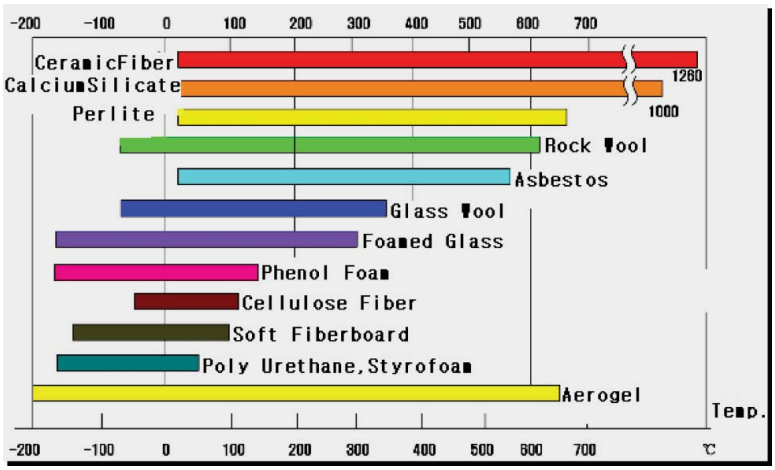

Figure 18. Applicable temperature ranges of insulations [57].

2.3.2. *Aerogel blanket Spaceloft® 3251*

For research into the possible advantages of laminated aerogel blankets for textile use, a silica aerogel blanket Spaceloft® 3251 (Aspen Aerogel, USA) was embedded in a non-woven made from polyester microfibres. The silica aerogel blankets produced dust on handling, because the brittle silica aerogel was crushed. The resulting fine dust is very oleophilic and gives an unpleasant feeling on contact with human skin. Because of this, aerogel blankets must be protected against the proliferation of dust into the surroundings when they are to be made into garments. The silica aerogel blanket was, therefore, laminated with a pre-prepared laminate of monolithic breathable membrane Platilon® M2234 made from polyether block amide (PEBA) (Bayer Material Science Co., Germany) and a fine warp-knitted fabric made from polyester filament yarns. Lamination of silica aerogel blanket was undertaken on industrial equipment in Zvezda SPT Kranj (Slovenia) using a hot-melt gravure procedure by dot bonding with reactive polyurethane. The aerogel blanket was laminated on both sides (Figure 19) to yield a five-layered composite [55].

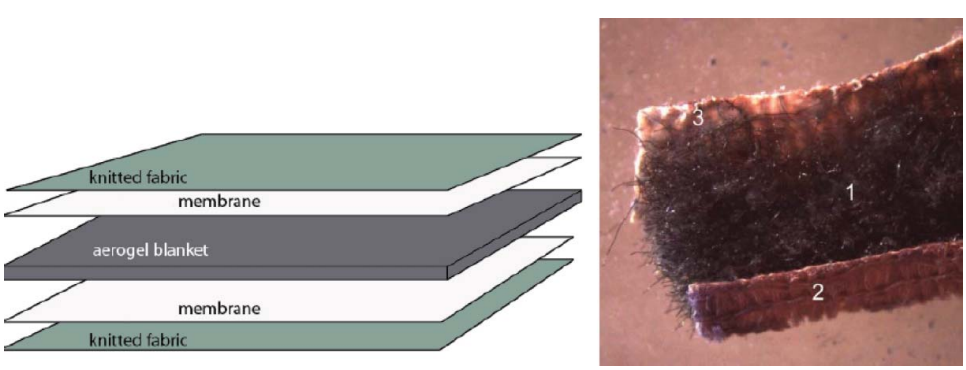

Figure 19. Left: Schematic diagram of a five-layered laminated silica aerogel blanket and its stereomicroscope view. Right: A cross section of laminated aerogel blanket: 1 — upper layer of knitted fabric, 2 — laminated aerogel blanket with membrane on both sides [55].

The thermal conductivity of the laminate, (λ_x), was determined using the device shown in Figure 2, where the heat flow through the sample and a reference plate with a known thermal conductivity (λ_n) was at equilibrium. The sample together with three copper plates for measuring temperatures T_1, T_2, and T_3, and a glass reference plate of thickness $dn = 4$ mm was placed between the upper hot and lower cold metal cylinders. The upper cylinder and a copper plate (T_3) loaded the sample with a pressure of 5.39 kPa. Thermal conductivity was calculated as follows [55]:

$$\lambda_x = \lambda_n \times \left(\frac{dx}{dn}\right) \times \left(\frac{T_2 - T_1}{T_3 - T_2}\right) \text{ (W/mK)} \tag{2.18}$$

where T_1 is the temperature between the aerogel blanket and membrane, T_2 is the temperature between the membrane and knitted fabric, and T_3 is the temperature above the knitted fabric, i.e. the temperature of the hot copper plate.

Silica aerogel blanket Spaceloft® 3251 is a flexible material of dark grey colour, with hydrophobic and oleophilic properties, and a thermal conductivity of 0.013 W/(mK) at 0 °C, and 0.016 W/(mK) at 100 °C [58]. It is made from non-woven polyester microfibres with an average diameter of 10 μm and a melting point of 236 °C. The grey colour of the aerogel blanket originates from the fibres and silica aerogel containing small metal particles to reduce the influence of thermal radiation from the environment. The silica aerogel is the matrix component in the Spaceloft® 3251 and is brittle and prone to crushing (see Figure 20), whereas the laminated silica aerogel blankets have been found to be easily cut, sewn, and glued, similar to non-woven materials. [55].

Despite the presence of additional layers, the laminated silica aerogel blanket is a very light material with volume density of only 0.205 g/cm^3. At a thickness of 2.51 mm, the mass per unit area was only 616 g/m^2, which is appropriate for using in outerwear garments for personal protection in extreme cold environment conditions. The thickness of the non-laminated aerogel blanket Spaceloft® 3251 was declared to be 3 mm, but in the laminate it was reduced to 2.51 mm, because in the lamination process the aerogel blanket was moved continuously between two heated rollers to apply the thermoplastic adhesive, exerting compression and bending forces that caused a significant crushing of silica aerogel and partial softening of the silica aerogel blanket. The technology employed in the experiments enabled only one-sided lamination per pass, so that the aerogel blanket had to be passed between the rollers two times to be laminated on both sides. The non-woven made from polyester microfibres embedded in the silica aerogel were unable to return to their original positions and thickness after the lamination process had taken place. The membrane protected the laminated aerogel blanket against losses of silica aerogel dust that emerged at bending but also allowed the laminated aerogel blanket water to remain vapour permeable and water resistant. The Platilon® thermoplastic polyurethane membrane (Covestro, Leverkusen, Germany) was also water vapour permeable, sufficiently extensible, mechanically resistant, and impermeable to aerogel dust [55], whereas the silica aerogel blanket Spaceloft® 3251 is hydrophobic and also a very oleophilic material (Figure 21). At 21 °C and 85% relative humidity, the laminated silica aerogel blanket absorbed only 2.39% of moisture [55].

The measured thermal conductivity of the laminated aerogel blanket Spaceloft® 3251 measured using the device shown in Figure 22 was 0.0474 W/(mK), a value which is

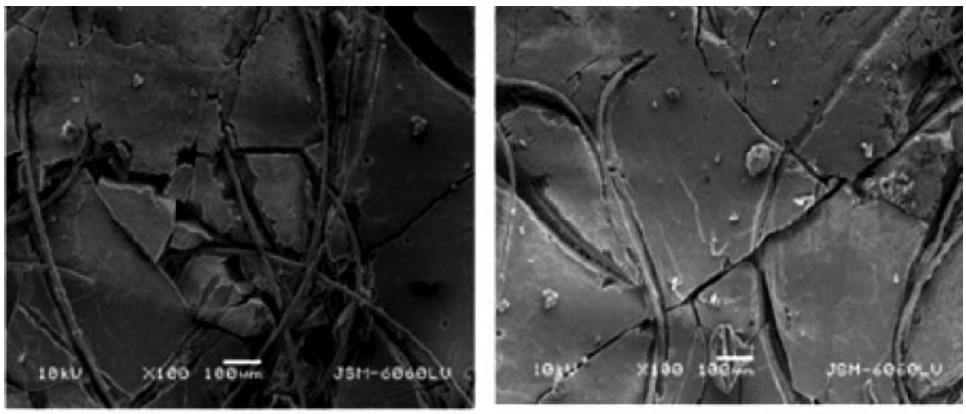

silica aerogel blanket Spaceloft® 3251 before lamination

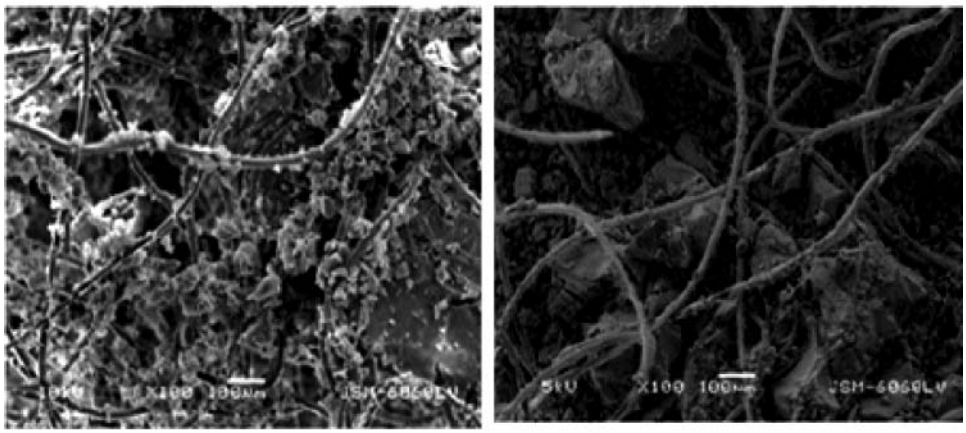

silica aerogel blanket Spaceloft® 3251 after lamination

Figure 20. Surface view of silica aerogel blanket; the upper views show cracks before lamination and the lower pair of images a much crushed structure of silica aerogel blanket after lamination and after removal of membrane with knitted fabric [55].

water drops on silica aerogel blanket surface

oil drops on silica aerogel blanket surface

Figure 21. Silica aerogel blanket Spaceloft® 3251; demonstration of hydrophobic properties (left) and oleophilic properties (right) [55].

Figure 22. Device for measuring thermal conductivity [55].

more than twice that of silica aerogel blanket, but comparable to that of classic thermo-insulative materials, such as Neoprene or Thinsulate [55].

2.3.3. Nanogel with aramid blended fabric

A 65/35 wool/aramid fibre blend fabric of areal density around 230 g/m^2 was coated with different percentages of Nanogel® (a super-hydrophobic, nanoparticulate silica aerogel from Cabot Corporation, Boston, MA) using an acrylic binder. Coated fabrics with 2%, 4%, and 8% aerogel were produced with an average viscosity of the coating paste of 20,000−30,000 centipoise. The coated fabrics were cured at 105 °C for 10 min, then their thermophysiological properties were analysed.

The thermal resistance of the fabric was measured according to ISO 11092: 1993 Textiles − Physiological effects − Measurement of thermal and water vapour resistance under steady-state conditions (sweating guarded-hotplate test), referred to as the 'skin model' (there is now a revised version, ISO 11092: 2014) (see Figure 23). This instrument is intended to simulate the heat and mass transfer processes which occur next to the surface of the skin [59,60]. Here, the thermal resistance (Rct) is the temperature difference between the two faces of a material divided by the resultant heat flux per unit area in the direction of the temperature gradient. Thermal resistance, expressed in m^2 K/w, where K is the temperature in degrees Kelvin, is a quantity specific to textile materials or composites. The thermal resistance (Rct) determines the dry heat flux across a given area in response to a steady applied temperature gradient. The specimen to be tested is placed on an electrically heated plate with conditioned air ducted to flow across and parallel to its upper surface as specified in ISO 11092.

For the determination of the thermal resistance of the coated fabrics, the heat flux through the test specimen was measured after steady-state conditions had been reached. Standard machine settings for the thermal resistance test were measurement unit temperature: 35 °C; thermal guards temperature: 35 °C; air temperature: 20 °C; air speed: 1 m/s; and relative humidity: 65% [61].

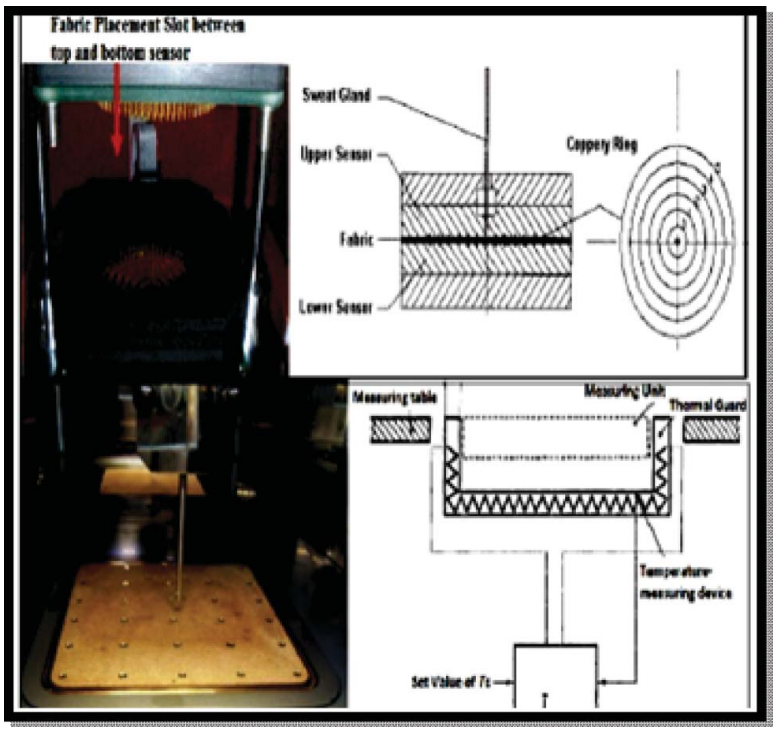

Figure 23. Measuring unit of the moisture management tester (MMT) (top) and sweating guarded hot-plate (bottom) [61].

Figures 24 and 25 show the fabric images for the 2%, 4%, and 8% aerogel-coated fabrics. For ease of presentation, the different fabric types used for the test purpose were coded as follows:

A1 : 2% aerogel, coated on the outer surface of the fabric;
$A1_{opst}$: 2% aerogel, coated on the 'next-to-skin' surface of the fabric;
A4 : 4% aerogel, coated on the outer surface of the fabric;
A8 : 8% aerogel, coated on the outer surface of the fabric.
B : fabric coated with paste containing all additives except the aerogel;
C : Uncoated fabric;
D : Gore-Tex® Airlock® fabric – composed of heat and chemical-resistant spacers made of foamed silicone on a Gore-Tex® moisture barrier (W. L. Gore Associates, Newark, DE).

After coating, along with measuring physical parameters like weight and thickness, fabric's microscopic images were also examined. The results for the physical parameters are shown in Table 6 [26] and the microscope images in Figure 25.

From the test results, it is clear that the aerogel particles on the fabric surface increase the thermal resistance of the fabric. The thickener-coated fabric has showed thermal resistance of 0.0118 m^2 K/W whereas the aerogel-coated fabric (A1) has showed thermal resistance of 0.0199 m^2 K/W. In other words, a 2% coating of aerogel provided a 68.64%

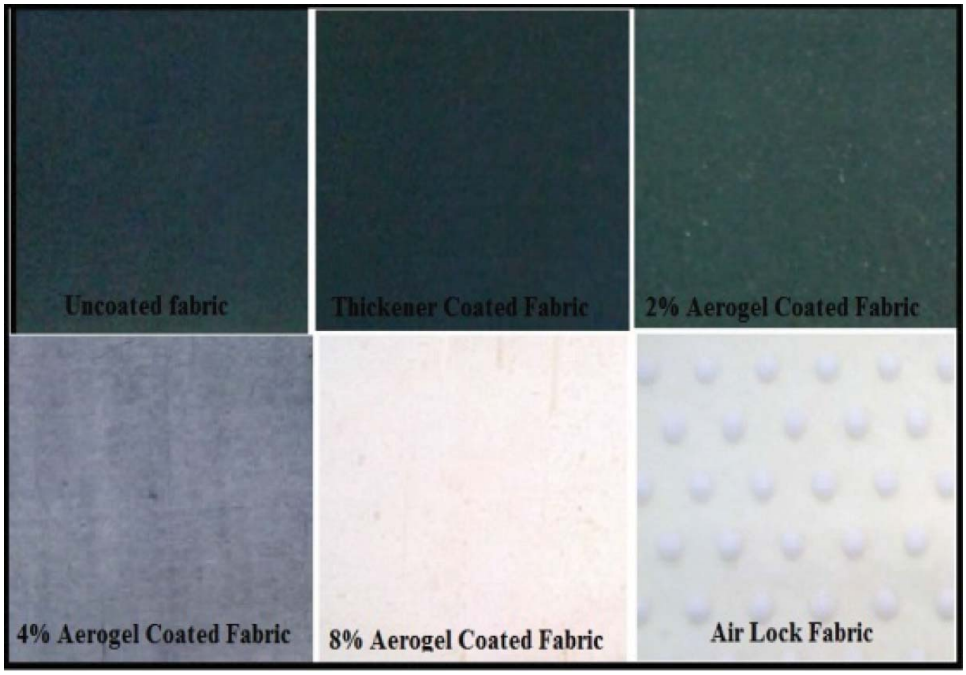

Figure 24. Different types of coated and uncoated fabrics [61].

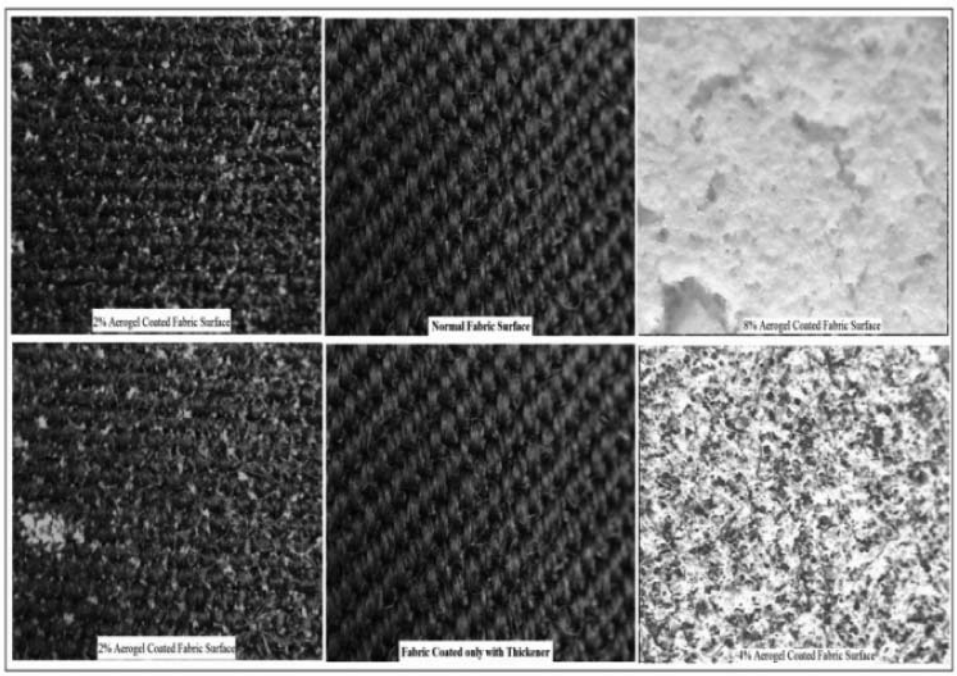

Figure 25. Microscopic view of some selected fabric samples: fabric tyspe A1, C, A8 (from top left) and A1, B, A4 (from bottom left) [61].

Table 6. Test result summary [61].

Fabrics	Thickness (mm)	Weight (g/m^2)	Air permeability (mL/cm^2/s)	Thermal resistance (m^2 K/W)
Al	0.47	236	64.3	0.0199
Al opst	0.47	236	64.3	X
A4	0.48	242	45.1	X
AS	0.68	X	10.2	X
B	0.47	235	111.6	0.0118
C	0.45	221	117.9	X
D	0.69	X	10.2	X

Note: X = Not tested.

increase in thermal resistance [61]. Due to aerogel coating, between 4% and 6% increases in thickness and a 6%–9% incremental increase in fabric weight per unit area were observed. Thickness increases the resistance to the transfer of heat and moisture. Previous research has shown that for two conventional fabrics of equal thickness, the lower density fabric shows the greater thermal insulation, but in this case, coating increased the density but resulted in higher insulation [61].

2.4. Assessment of thermal improvements gained by using aerogels in garments

Thermal images using IR photography have been used to look for thermal shorts in prototype aerogel garments and for comparing their thermal performance with commercial garments. Figures 26–29 show IR comparisons at various suit orientations. Prior to capturing these IR photographs, a human test subject had stood in a dry test chamber conditioned to an air temperature of −10 °C (14 °F) for 30 min while wearing each garment. Note that the colour coding for surface temperatures is shown on the right-hand bar in each photograph. The temperature is given in degrees Fahrenheit and localized surface temperatures on different parts of the garment are indicated for reference.

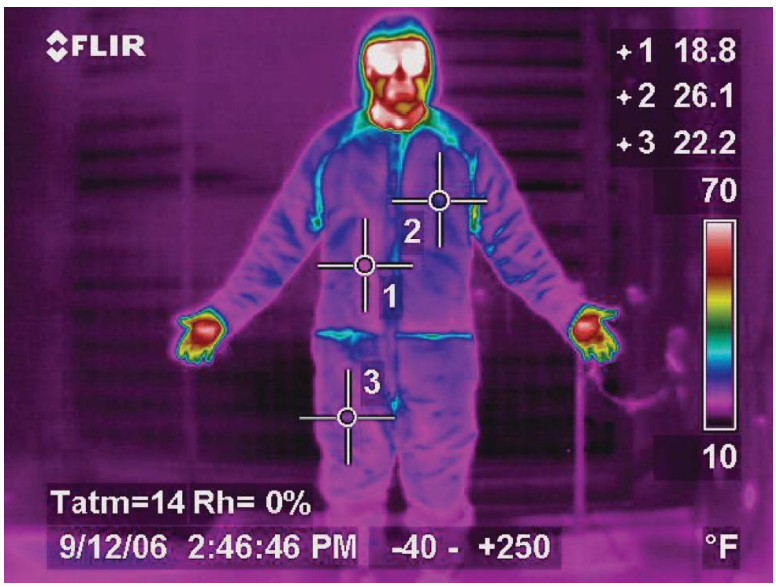

Figure 26. Frontal view of prototype aerogel garment. Typical surface temperatures 18–26 °F [62].

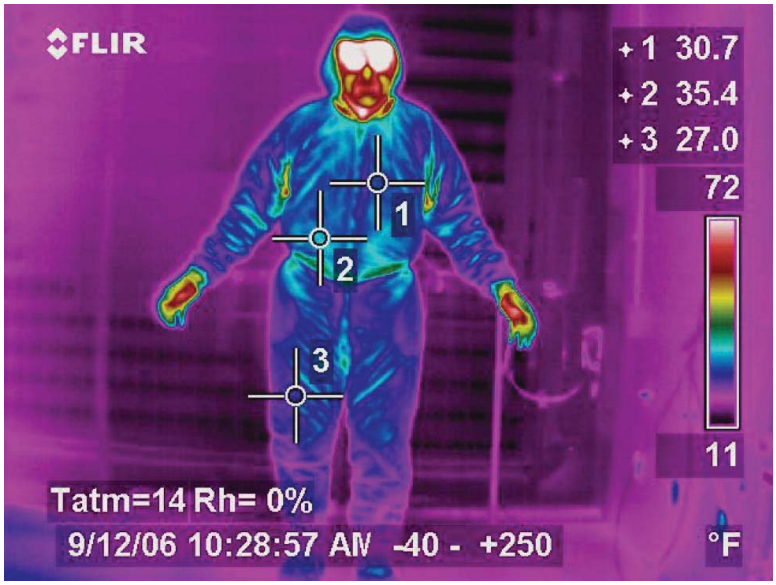

Figure 27. Frontal view of 400-g Thinsulate garment. Typical surface temperatures 27–35 °F [62].

The aerogel-infiltrated fabrics can be seen to provide superior thermal protection in comparison with the garment constructed from commercially available microfibrous polypropylene batts. Comparing Figures 26 and 27, the outer surface temperatures for a garment constructed with microfibrous polypropylene batts show up as warmer in the frontal view than the aerogel garment, indicating higher heat loss from the garment constructed using the microfibrous polypropylene batts. In general, the surface temperatures on the commercial garment can be seen to be consistently higher in all views when

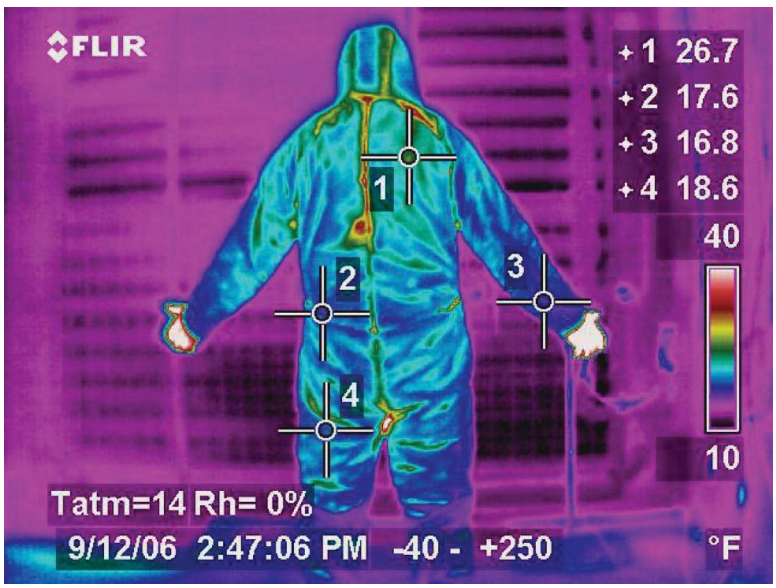

Figure 28. Back view of aerogel garment. Typical surface temperatures 17–27 °F [62].

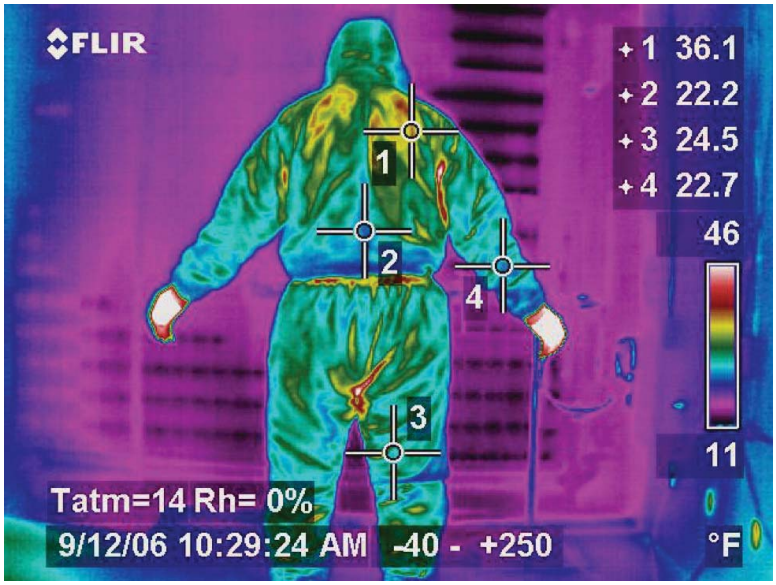

Figure 29. Back view of 400-g Thinsulate garment (surface temperature range 22−36 °F) [62].

compared to the aerogel garment [62]. The front views are shown in Figures 26 and 27 and back views are shown in Figures 28. and 29.

Additional to demonstrating superior thermal protection, the thermal performance of composite aerogel garments has been shown to be minimally affected by either machine or hand laundering. Laundering was done using either a weak bleach solution or a non-ionic detergent. Air-drying gave the best results in this investigation, as substantial shrinkage of the encapsulated aerogel panels was observed during machine drying.

Laboratory testing has shown specific insulation values for aerogel batt materials to approach 12 clo. Prototype aerogel garments have been characterized to provide a thermal improvement of 76% when compared to a 400 g Thinsulate^{TM} ensemble during submerged thermal manikin testing (2.22 clo for the aerogel garment versus 1.26 clo for 400 g Thinsulate^{TM}). The aerogel garment had approximately the same thickness and weighed approximately 0.2 kg more than the Thinsulate garment. In comparison, 400 g Thinsulate, a standard for cold weather clothing, has a specific insulation value of approximately 5 clo per inch which changes significantly when compressed. IR thermal imaging confirmed lower heat loss from the aerogel garment during surface exposures to cold air environments. Thermal conductivity testing indicates that this superior thermal performance is minimally impacted by repeated flexing and compression, or when subjected to complete water immersion [62].

2.5. *Thermal properties of SiO_2 aerogel composites reinforced with electrospun PVDF webs*

The thermal conductivities of SiO_2 aerogel composites reinforced with the electrospun Polyvinylidene fluoride (PVDF) webs with three different microstructures were measured at room temperature. The microstructures were

Table 7. Thermal conductivity of aerogel composites supported by electrospun PVDF [63].

Microstructure type of electrospun PVDF	Thermal conductivity of aerogel composites (W/m//K)
Microparticle	0.039
Microparticle/nanofibre	0.032
Nanofibre	0.027
Without PVDF (pure aerogel)	0.024

(1) aerogel composites reinforced with the electrospun PVDF nanofibres (best insulator);
(2) aerogel composite reinforced with PVDF microparticles (poorest insulator);
(3) aerogel composite with a combination of PVDF microparticles and nanofibres (intermediate insulation performance).

It was observed that the thermal conductivity of the electrospun PVDF nanofibrous webs was significantly reduced from 0.037 and 0.027 W/m/K by filling the electrospun PVDF nanofibrous webs with SiO_2 aerogel (Table 7). It is because the pores of the electrospun PVDF nanofibrous webs at the micron scale were filled with and separated by the aerogel into smaller pores of nanometre scale. The improvement in insulating ability was brought about because the gaseous thermal conductivity of the electrospun PVDF webs filled with nanoporous aerogel had been significantly reduced – the size of the aerogel nanopores was smaller than that of the molecular free path of the air in the pores and this had brought about the reduction. As a result, the aerogel composites reinforced with the electrospun PVDF webs had lower thermal conductivity than the electrospun PVDF webs alone. The aerogel composites reinforced with the electrospun PVDF nanofibres yielded the lowest thermal conductivity of 0.027 W/m/K in all the three aerogel composites. The composite aerogel reinforced with the PVDF microparticles had the highest thermal conductivity of 0.039 W/m/K, and the composite with a combination of PVDF microparticles and nanofibres had a moderate thermal conductivity of 0.032 W/m/K. The form of the PVDF in the composite is important, because the electrospun nanofibres had smaller diameters and greater specific surface area (SSA) which is advantageous to shield the heat radiation and reduce the effective thermal conductivity/increase the insulation ability [63].

It can be observed that the SiO_2/aerogel composites have greater thermal stability below 475 °C but poorer thermal stability above 475 °C than the pure SiO_2 aerogel. The pure aerogel showed approximately 10% weight loss in the temperature range of 350–475 °C (loss which is derived from the degeneration of $Si-O-C_2H_5$ groups). The aerogel composites reinforced with the electrospun PVDF webs showed significant weight loss in the temperature range of 450–510 °C owing to the degeneration of the PVDF. The weight loss at 510 °C of the three aerogel composites: reinforced by nanofibres, combined microparticles/nanofibres, and microparticles was 60%, 44%, and 34%, respectively.

Table 8 shows the crack behaviour of SiO_2 aerogel composites reinforced with the electrospun PVDF webs; in addition to showing the best insulating ability, the aerogel composites reinforced by PVDF nanofibres also showed better stability than those reinforced by PVDF microparticles. However, it should be noted that PVDF materials, including the electrospun PVDF webs, may melt at 172 °C without any noticeable weight loss; hence the SiO_2 aerogel composites reinforced with electrospun PVDF are only suitable for the application in thermal insulation below 172 °C [63].

Table 8. Properties of SiO_2 aerogel composites reinforced with electrospun PVDF webs [63].

Concentration of PVDF solution (wt%)	SiO_2 aerogel composites reinforced with electrospun PVDF web		
	Density	Integrity	Flexibility (g/cm^3)
18	Crack	Fragile	0.277
23	Intact	Flexible	0.235
29	Intact	Flexible	0.202

2.5.1. *Morphologies of SiO_2/aerogel composites reinforced by electrospun PVDF webs*

Figure 30 shows optical and scanning electron microscope images of SiO_2 aerogel composites reinforced with the three electrospun PVDF webs of differing microstructure. The SiO_2/aerogel composites were cut into 12-cm-diameter circles. It was observed that the SiO_2/aerogel composite specimens reinforced with the electrospun PVDF nanofibres and those with combined PVDF microparticles and nanofibres maintained their integrity at a large diameter size of 12 cm, significantly bigger than that in the previous literature [64]. From Figure 30(e) and 30(f), the SiO_2/aerogel composite specimens reinforced with the electrospun PVDF nanofibres and with combined PVDF microparticles and nanofibres showed good flexibility even if they were bent into a cone shape. It was the first time that

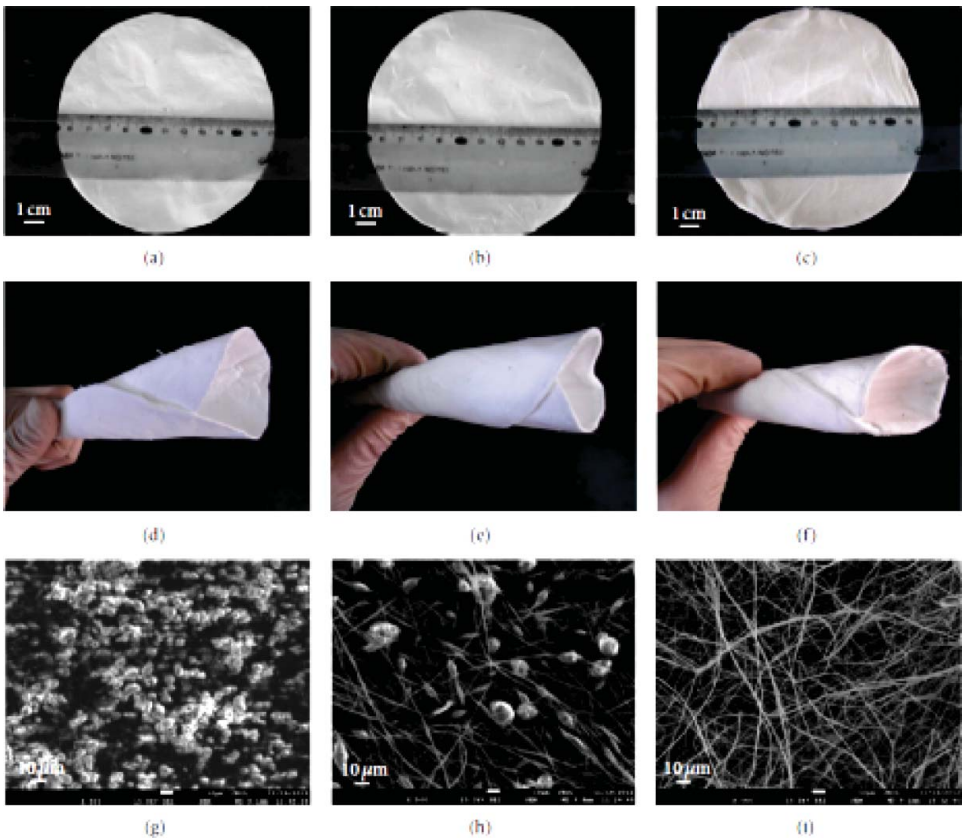

Figure 30. Morphology and microstructure of the three electrospun PVDF webs (a, d, and g) microparticles electrospun from 18 wt% PVDF; (b, e, and h) combined microparticles and nanofibres electrospun from 23 wt% PVDF; (c, f, and i) nanofibres electrospun from 28wt% PVDF [63].

such intact and flexible SiO_2/aerogel composite specimens reinforced with the electrospun PVDF nanofibres and with combined PVDF microparticles and nanofibres had been achieved. By comparison, the SiO_2/aerogel composite specimen reinforced with electrospun PVDF microparticles (Figure 30(a)) was relatively stiffer and developed some microcracks while being bent [63].

The morphologies of the aerogel composites reinforced with the three microstructured PVDF webs are shown. The intact morphology of the aerogel composites reinforced with PVDF nanofibres compared with the cracked morphology of that reinforced with PVDF microparticles imply that the electrospun PVDF nanofibres effectively improved the strength and the flexibility of the aerogel. It is likely to be because the electrospun PVDF nanofibres absorb the destructive energy and maintain the integrity of aerogel composite specimens. The second reason is that the diameter of the PVDF nanofibres is around 20−200 nm which is much closer than the dimensions of the microparticles to the size of holes and particles of the SiO_2 aerogel. For the aerogel composites reinforced with electrospun PVDF nanofibres, the induced tension differences between the interfaces of the nanofibres and the aerogel are expected to be reduced and the defects from bending were correspondingly decreased. As a result, the aerogel composites reinforced with electrospun PVDF nanofibres exhibited better flexibility than either the pure SiO_2 aerogel or the SiO_2 aerogel composites reinforced with electrospun PVDF microparticles. Figure 31 shows the contact angle of the pure aerogel and the aerogel composites reinforced with electrospun PVDF webs. Whilst the contact angle of the pure aerogel is 139.0°, the contact angle of the aerogel composites was slightly reduced to between 128.5° and 134.1° with the electrospun PVDF webs added. It may be because the added electrospun PVDF microparticles or nanofibres increase the surface roughness of the aerogel. The SiO_2 aerogel composites reinforced with electrospun PVDF microparticles were still fully hydrophobic to water, so the aerogel composites could retain their thermal insulation even in moist environments [63−66].

2.6. Heat insulation performance and mechanics of cellulose/SiO_2 composite aerogels

In order to analyse the effect of density and porosity on heat insulation performance, different densities and porosities of a cellulose/SiO_2 composite aerogel were obtained by using a variety of SiO_2 contents and cellulose concentrations. Density and porosity measurements of the resulting cellulose−SiO_2 composite aerogel with different SiO_2 content and cellulose concentration are shown in Table 9.

As the SiO_2 content was increased, the number of SiO_2 particles which filled up the pores of aerogel increased and the silica aerogel layers became thicker; the porosity was reduced accordingly as shown in Figure 32. The decrease in the porosity was a direct reflection of the increased density of the polymer network.

Density and porosity are the main factors influencing the heat insulation performance of bulk materials [65]. Generally speaking, the thermal conductivity of a dense solid is always higher than that of still air, and at normal temperatures, thermal conductivity increases with the increase of the mass of solid matter content in unit volume.

As shown in Figure 33(a), with increasing density, the thermal conductivity also increases. Although SiO_2 has a substantially low density and has a negligible effect on

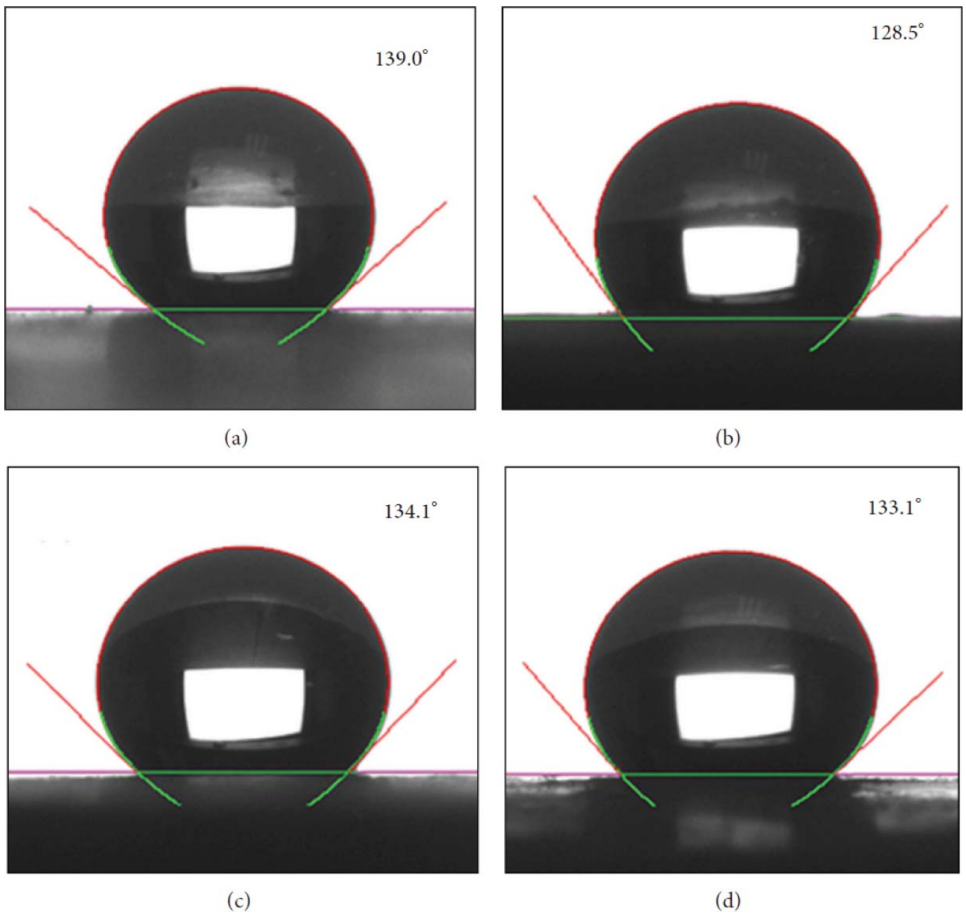

Figure 31. Contact angles between water and aerogel and aerogel composites reinforced with electrospun PVDF webs: (a) pure aerogel; (b) aerogel composites reinforced with electrospun PVDF microparticles; (c) aerogel composites reinforced with electrospun PVDF nanofibres; (d) aerogel composites reinforced with electrospun PVDF microparticles and nanofibres [63].

conductivity, composites with SiO_2 show higher densities and relatively higher thermal conductivity [66]. The higher the porosity, the lower the thermal conductivity, as shown in Figure 33(b). The lowest thermal conductivity, 0.0257 W/(m K), can be achieved with a density of 0.233 g/cm^3 and a porosity of 75.97%. An increase in porosity can reduce the mean free energy, and thus reduce the thermal conductivity of composite aerogel materials.

Table 9. Density and porosity of the resulting cellulose−SiO_2 composite aerogel with different SiO_2 content and cellulose concentration [145].

Sample	CS1	CS2	CS3	CS4	CS5	CS6	CS7	CS8	CS9
Concentration of cellulose solution (%)	5	5	5	5	5	5	2	3	4
SiO_2 content (%)	9.95	10.85	13.66	14.14	14.26	16.25	7.25	8.76	12.36
Density (g/cm3)	0.31	0.34	0.26	0.26	0.36	0.45	0.23	0.35	0.41
Porosity (%)	20.09	15.33	37.50	21.93	21.72	22.12	75.97	29.42	22.29

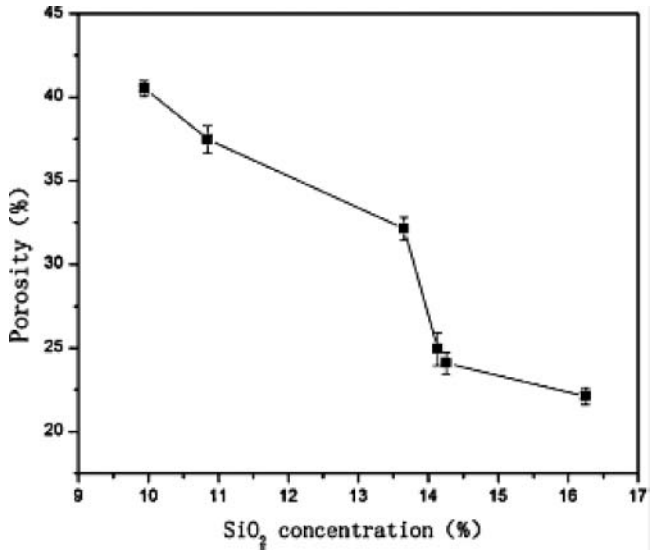

Figure 32. Effect of SiO_2 concentration on porosity of composite aerogel at 5% cellulose concentration [145].

The thermal conductivity of both cellulose aerogel and cellulose−SiO_2 composites increased with the increase of cellulose concentration as shown in Figure 34. Limited by the solubility of cellulose in solvent, when the cellulose concentration reached a critical level, the amount of undissolved cellulose increased and the absolute content of cellulose also increased. Thus thermal conduction in solid and the thermal conductivity increased accordingly. When the cellulose concentration was 3% in cellulose aerogel and was 2% in cellulose−SiO_2 composite aerogel, the thermal conductivity reached the lowest point because, limited by the cellulose concentration, 2% cellulose aerogel had less cellulose involved in forming the structure of aerogel, which caused the structure of aerogel to be incomplete. However, a 3% cellulose aerogel had a relatively completed structure, and the lower density of 0.233 g/cm3 and higher porosity of 84.88%. So the 3% cellulose aerogel showed the lowest thermal conductivity of the cellulose aerogels. Although the same

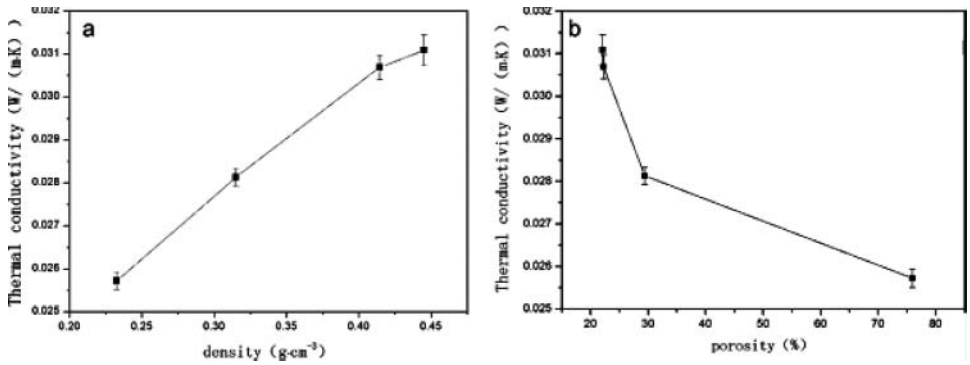

Figure 33. Effect of density and porosity of cellulose/SiO_2 composite aerogel sample number CS7 on its thermal conductivity [145].

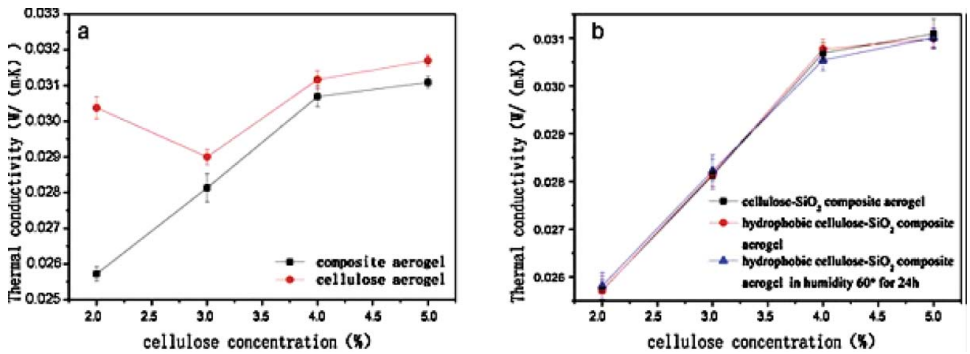

Figure 34. Effect of cellulose concentration on the thermal conductivity of cellulose/SiO_2 sample number CS7 compared with a 5% cellulose aerogel [145].

problem occurred in composite aerogels, and a 2% cellulose could not offer a complete structure, huge amounts of SiO_2 particles and silica aerogel filled up into aerogel, which provided an effective support and a stable structure in the composite aerogel, and because the SiO_2 particles and silica aerogel had low density and low thermal conductivity [67], it resulted in a 2% cellulose content yielding the lowest thermal conductivity. Generally, the thermal conductivity of composite aerogels was lower than that of cellulose aerogel. On the one hand, because of the low thermal conductivity of SiO_2, the composite aerogel also had a lower thermal conductivity. On the other hand, the thermal resistivity of open porous composite aerogel was also increased when its effective pore size decreases. The mean free motion path of air molecule is about in 70 nm [68]. After the formation of the SiO_2 composite, the number of pores which met the size required to limit motion was increasing. In materials, thermal conduction through the small size of the connections between the particles makes up the conduction path and when the pore size is comparable to or smaller than the mean free path of the gas, the molecules of the latter collide more often with the molecules forming the solid part than amongst themselves. In fact, the gas molecules will tend to stick to the molecules of the solid part, virtually eliminating thermal conductivity through the gas inside the material.

With increasing cellulose concentration, the internal pore size of the composite aerogel increases while the number of pores less than 70 nm decreases. Therefore, the thermal conductivity of the composite aerogel increases as its cellulose content is raised.

Cellulose/SiO_2 composite aerogel is a kind of porous insulating material composed of a solid phase (crystalloid and non-crystalloid) and gas phase (pore). The solid matrix of the composite aerogel is formed by interconnection of cellulose molecule clusters. There are a lot of air molecules in the interstices of cellulose aerogel. The heat transfer in aerogels can be divided into solid-phase heat conduction and gas-phase heat conduction [69].

In the case of solid-phase heat conduction, non-metallic crystalline materials conduct heat by the transport of quantized atomic lattice vibrations called phonons. Thermal conductivity depends on how far phonons travel between scattering events – their mean free paths. Due to the breadth of the phonon mean free path spectrum, nanostructuring of materials can reduce thermal conductivity from bulk by scattering long mean free path phonons, whereas short mean free path phonons are unaffected [70]. The solid heat transfer in aerogels is mainly determined by the mean free path of phonons in the solid

structure unit. During the step in aerogel formation involving dissolution of the cellulose, non-crystalline areas and crystalline areas are both opened. Thus the transfer space for phonons [71] enlarges. At the same time, the size of the solid particles also influences the density of the aerogel to a certain degree. The composite aerogel with a relatively low density has quite small solid particle sizes, so the phonon mean free path is reduced and thermal conductivity is decreased.

At medium and low temperatures, gas molecules in random motion in air have different average kinetic energies in different areas of a material [72]. Given that the air cannot simply flow on account of its density differences at different temperatures, when the high-energy molecules move from a high- to a low-temperature area, their energy is transmitted by molecular collision and heat is conveyed in that way. Heat conveyance by a large quantity of molecules is expressed as macro-heat conduction. The mean free path of a gas molecule in air influences the ability of molecules to exchange energy on an infinitesimal surface in space, and this influences the heat insulation performance of the composite aerogel further. The low density and high porosity of composite aerogel pose multiple restrictions to the movement of the gas molecules. In forming the cellulose/SiO_2 aerogel composite, the number of pores less than 70 nm is increased, so the flowability of the gas is reduced causing the gas-phase heat conduction to reduce too, leading to a relatively low thermal conductivity of the gas phase. Therefore, as a consequence of the effects imposed by its combination of low density and high porosity, the cellulose/SiO_2 composite aerogel exhibited excellent heat insulation performance.

2.6.1. Hydrophobic modification of cellulose/SiO_2 composite aerogels

The conclusion from Fourier transform infrared spectra was that the presence of SiO_2 in the cellulose/SiO_2 composite aerogel could improve the hydrophobicity of the composite aerogel. Besides possessing a relatively large SSA and a porous structure, the composite aerogel was rich in hydroxyl groups, so it easily adsorbed water vapour from the air and gathered water on its surfaces or in pores. Water has a much higher thermal conductivity than air (approximately 21 times greater) [73]). If water molecules were to be adsorbed by the cellulose/SiO_2 composite aerogel, its thermal conductivity would be increased, and its heat insulation performance reduced. As shown in Figure 35, for the composite aerogel

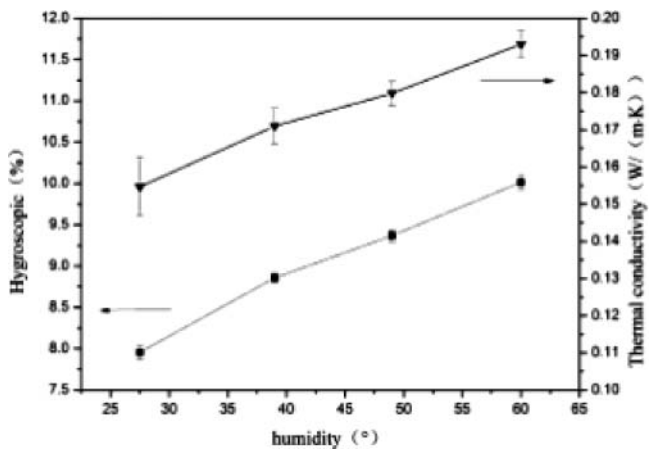

Figure 35. Effect of air humidity on hygroscopicity rate and thermal conductivity of sample CS7 [145].

with 2% cellulose concentration, its hygroscopicity increased with a rise in humidity, while the thermal conductivity also increased significantly with a rise in humidity. In order to obtain stable heat insulation performance of composite aerogel over a variety of environmental conditions, a practicable way was to improve its hydrophobicity. Cold plasma modification technology was employed to modify the surface of the composite aerogel from hydrophilic to hydrophobic using carbon tetrachloride.

The modification process mainly involved chlorination. It was deduced that the CCl_4 molecule was dissociated by electronic impact under the electrical discharge. The process of CCl4 gas dissociation was the same as that for carbon tetrafluoride (CF_4) dissociation [74]. The CCl_4 molecules are dissociated by electron collisions as follows:

$$\begin{aligned} e + CCl_4 &\rightarrow e + CCl_3 + Cl \\ e + CCl_4 &\rightarrow e + CCl_2 + 2Cl \\ e + CCl_3 &\rightarrow e + CCl_2 + Cl \\ e + CCl_2 &\rightarrow e + CCl + Cl \\ e + CCl &\rightarrow e + C + Cl \end{aligned} \tag{2.19}$$

During the process, the CCl_x radicals acted as functionalization agent, and of these, CCl_2 had the most density in plasmas, relative to which, chlorine atoms played the role of etching agent and had the least density in the plasmas.

The effects of using different discharge powers and durations on the change in water contact angle on the composite aerogel surface were examined and are shown in Figure 36. Under 50-W treatments, a 5-min treatment time, increased the water contact angle of the composite aerogel from 0° to 83°; after 10 min, the water contact angle was beyond 90°, and the surface of composite aerogel became hydrophobic; small increases in the water contact angle were then observed for treatment times beyond 20 min and a discharge power of 50 W and treatment time of 25 min yielded the largest contact angle of 132°. The outcomes at 70 W discharge power and a 25-min treatment time, however, were different. Whereas when the discharge power increased from 0 to 50 W, the water contact angle had increased and the trend to hydrophobicity had also increased, raising the discharge power to 70 W causing the water contact angle to begin to decrease. A

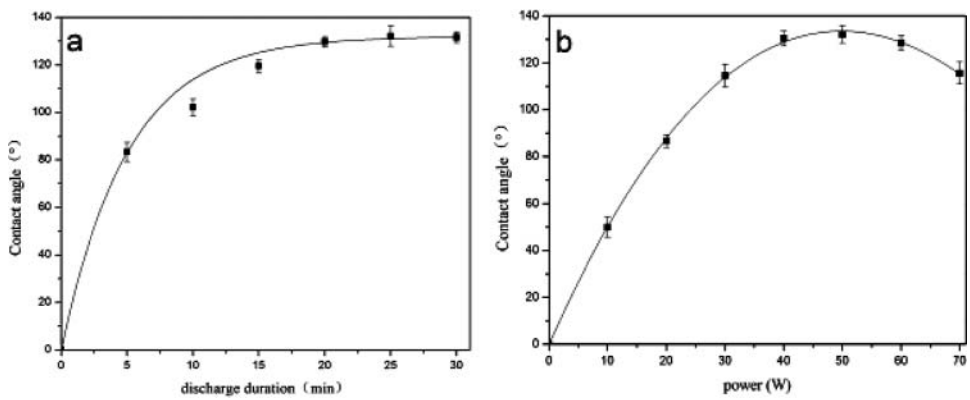

Figure 36. Effect of discharge duration and discharge power on water contact angle of sample number CS7 treated by CCl_4 plasma [145].

possible reason was that when composite aerogel was exposed to the more severe discharge conditions, sputtering or etching functions took the leading role instead of chlorinated grafting causing a reduction in the proportion of the carbon–chlorine functional groups formed.

The thermal conductivities of the composite aerogel before and after hydrophobic modification were compared and showed no significant difference. There was no significant change in the thermal conductivity of the hydrophobic composite aerogel after conditioning at a humidity of 60% for 24 h whereas the unmodified aerogel became more thermally conductive. It demonstrated that the plasma hydrophobic modification was useful, not just for improving the hydrophobility of composite aerogel surface, but also it would not reduce the excellent heat insulation performance shown by the dry composite aerogel and would allow this high level of performance to be maintained under humid conditions. Overall, plasma modification technology is an effective method of modifying the surface properties of the cellulose/SiO_2 composite aerogel.

2.7. Aerogel materials derived from polymers other than silica

Essentially, any liquid can be gelled whenever a continuous solid lattice structure is formed within the liquid phase, entraining the solvent within open pores. The key to making a nanoporous aerogel involves developing a balance between polymer chain growth and interchain cross-linking to yield the desired pore structure and high surface area. The modulus (stiffness) of the resulting cross-linked gels must be high enough to resist the capillary forces generated during solvent removal. This property is strongly influenced by the number of links between neighbouring chains per unit volume of gel. Many materials can be incorporated into the silica or metal oxide matrix at the sol stage, including organic polymers capable of modifying the aerogel's physical properties. Many highly cross-linked polymer systems can also be induced to create gels in organic solvents, such as resorcinol–formaldehyde (RF) resins, melamine–formaldehyde resins, polyimides, polyurethanes, polyisocyanurates, and various unsaturated hydrocarbon compounds.

2.7.1. Carbon aerogels

Carbon aerogels, or porous carbons synthesized via the sol–gel route, are considered to be interesting materials for high-temperature thermal insulation in non-oxidizing atmospheres or in vacuum [75, 76]. Carbon aerogels are open, porous solids consisting of a 3D network of spherical, interconnected, primary particles. The mean pore dimensions and particle size can be specifically adjusted to be in the range from several nanometres to a few micrometres by varying the synthesis conditions. Porosities of up to 99% can be achieved, making carbon aerogel suitable for thermal insulation applications, particularly at high temperatures, and also for electrodes in supercapacitors and gas diffusion layers in fuel cells [77, 78]. Carbon aerogel is often produced using RF as the main precursor, prepared by polycondensation of resorcinol with formaldehyde in an aqueous solution. Sometimes, sodium carbonate, which acts as a base catalyst, is mixed with resorcinol and deionized water, to accelerate dehydrogenation of resorcinol, and after stirring the solution for a few minutes, formaldehyde is added slowly into the solution to form a sol [79].

An overall preparation route for carbon aerogel beginning with a precursor gel prepared in this way is shown in Figure 37 and a series of typical processing routes are listed for preparing carbon aerogel.

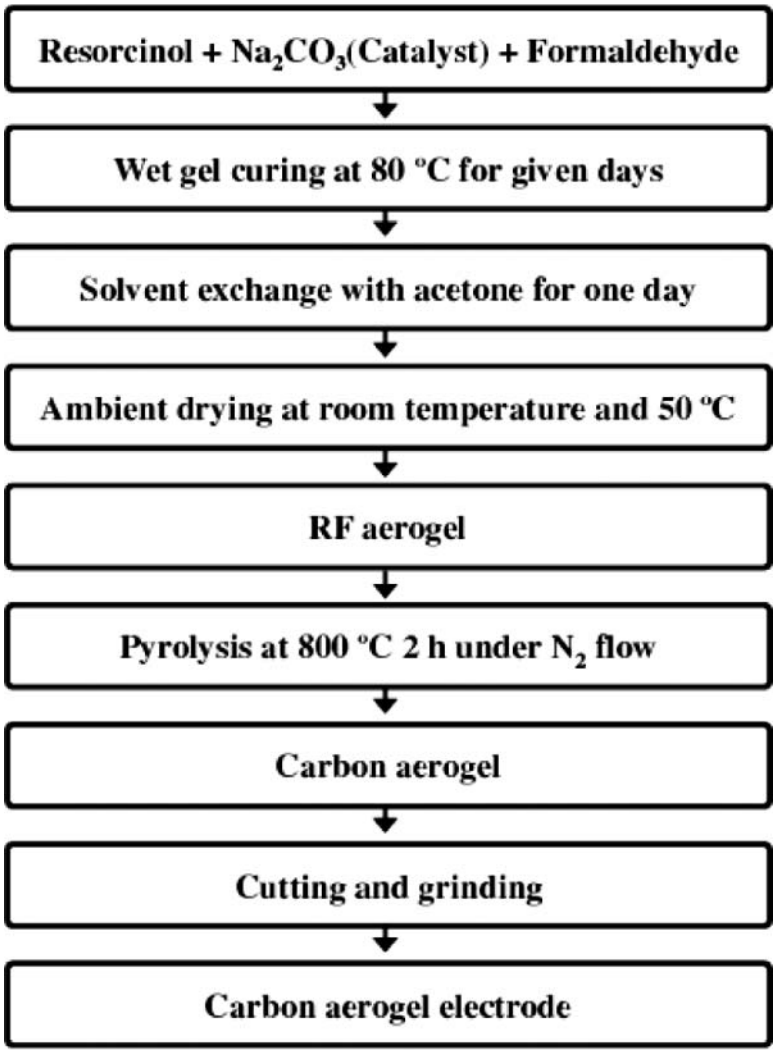

Figure 37. Overall preparation route for carbon aerogel [79].

Wiener et al. [80–82] investigated the high-temperature insulation properties of carbon-based aerogels derived via pyrolysis of the organic aerogel precursor synthesized using RF. The mass ratio of the RF reactants to water in the starting aqueous solution was adjusted to 25% (where the mass ratio = mass of RF to total mass of the solution) to yield a density of the resulting aerogel of about 230 kg/m^3. Equimolar quantities of RF were used. Following initial gel formation, the samples were exposed to a temperature of 85 °C for 24 h to allow further gelling and curing. The liquid within the pores of the wet gel was then replaced by ethanol to reduce the surface tension upon drying, subsequent to which, the gels were dried under ambient conditions. Finally, the resulting organic aerogels were pyrolysed in an argon atmosphere at 1073 and 2073 K. Figure 38 shows the microscopic structure of one of the carbon aerogels synthesized [79].

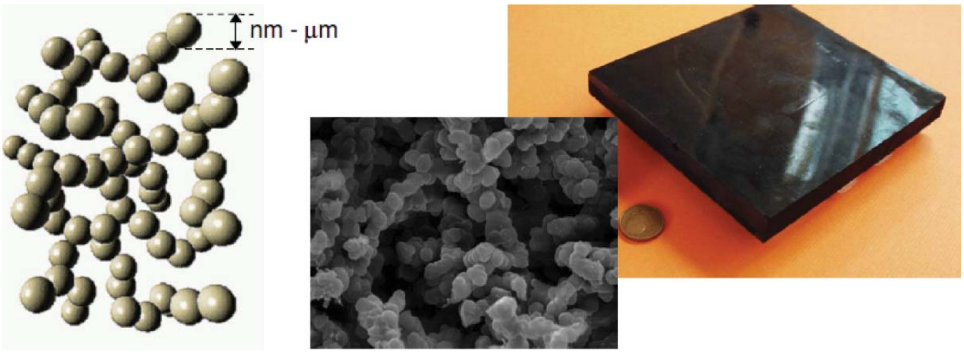

Figure 38. Left: Schematic representation of a carbon aerogel backbone; centre: SEM image of a carbon aerogel; right: macroscopic view of a carbon aerogel tile [89].

In the case of classical type of sol–gel-derived porous carbons synthesized from an aqueous solution of RF[83–88], whereas the concentration of the two reactants in the starting solution determines the meso- and macroporosity of the resulting porous carbon, it is the catalyst employed and its concentration that controls the size of the interconnected particle-like entities that form the carbon backbone (Figure 38). The thermal conductivity of a porous solid is essentially given by the superposition of the contribution of the heat transfer along the solid phase, the transport within the gaseous phase (pores), and radiative heat exchange. While at low temperatures, the heat transfer via the solid and the pore phase dominates, these contributions become only a minor effect at high temperatures where heat transport via radiation is the dominant factor. Materials such as carbon which show a high degree of opacity to IR radiation are, therefore, expected to be the best performers in providing insulation at high temperatures. In fact, carbon aerogels are extremely 'black' in the IR spectrum, reflecting only 0.3% of the radiation between 250 nm and 14.3 µm.

Depending on the felt density, the orientation of the fibres and the presence of additional connections between the fibres as a result of stabilization by pyrocarbon deposits, the available materials cover a range in thermal conductivity (Figure 39). The same plot shows the thermal conductivity of carbon aerogel as determined from the thermal diffusivity measured via a laser flash experiment and the heat capacity c_p determined with a differential scanning calorimeter [89]:

$$\lambda = a \quad \rho \quad c_p \tag{2.20}$$

The dark, filled-in symbols represent the thermal conductivity at ambient air pressure, while the hollow symbols indicate the figures obtained for the materials under vacuum. The dashed lines in the case of the aerogel mark the expected range in thermal conductivity at high temperatures where no experimental values are yet available. While at temperatures below 500 °C, the aerogel yields values for thermal conductivity that are within the same range as those for the best felts, the sol–gel-derived carbon aerogel shows a factor of up to four times better insulation properties for temperatures beyond 1500 °C. These attractive features are accompanied by mechanical stability providing self-supporting properties to the carbon aerogel and easy machining. Carbon aerogel is, therefore, expected to become one of the preferred materials for high-temperature thermal insulation. The SEM image of carbon aerogel is shown in Figure 40.

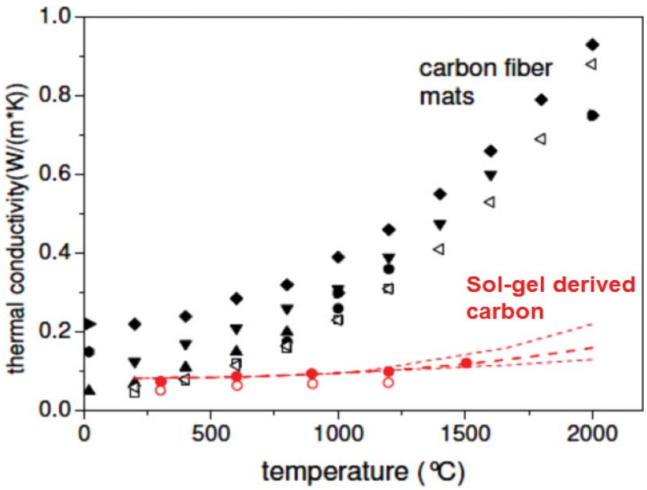

Figure 39. Total thermal conductivity of commercially available carbon fibre felts for thermal insulation (black symbols) and a carbon aerogel [89].

The effective thermal conductivities of carbon aerogel according to the determined values of thermal diffusivity, specific heat, and sample densities are shown in Figure 41 [90] for the two carbon aerogels investigated. Comparison of the values derived in a 0.1-MPa argon atmosphere and under vacuum shows that the difference between the two datasets is almost temperature independent and of the order of 0.02 W/m/K. This difference in thermal conductivities represents the contribution that the argon gas in the pores of the aerogel is making to the total effective thermal conductivity. In Figure 41, these data are compared to the experimental data of the total effective thermal conductivities measured in vacuum. The plot reveals that even at 1770 K, radiative transport makes only a small contribution to the total effective thermal conductivity of the carbon aerogel investigated [79]; indeed, the thermal transport by the heat transfer via the solid phase is rather

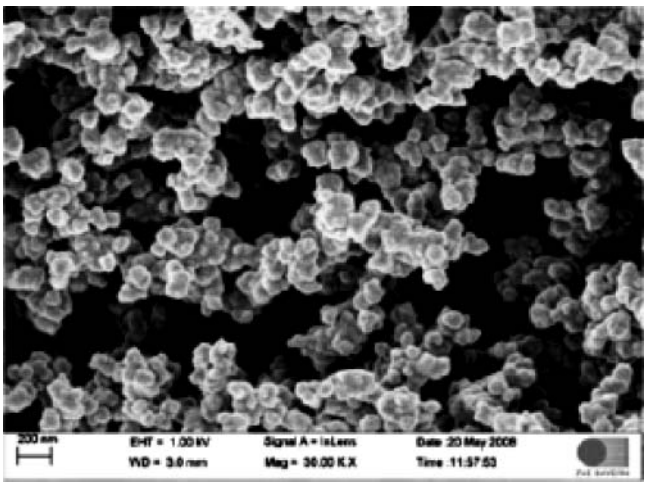

Figure 40. SEM image of one of the carbon aerogels ($T_{pyro} = 2073$ K) [90].

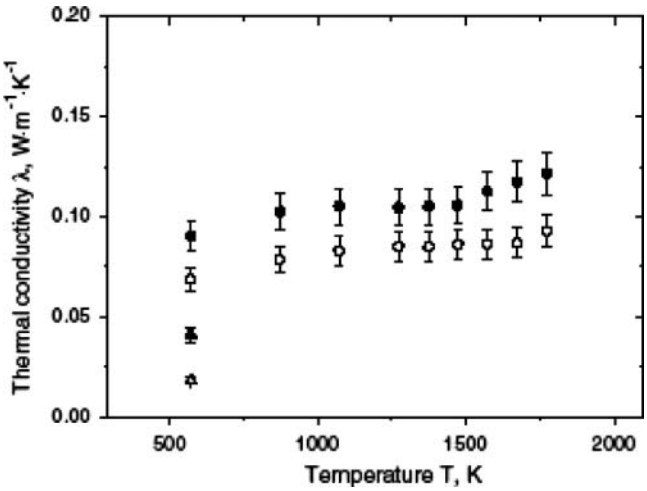

Figure 41. Thermal conductivity of the investigated carbon aerogel [90].

dominant. The full line in Figure 42 corresponds to a fit of a superposition of the radiative thermal conductivity and the solid thermal conductivity, whereas the upper dashed line in Figure 41 represents the effective thermal conductivity to be expected for a carbon aerogel derived from the same organic precursor as the samples measured here, but pyrolysed at a temperature of 2773 K. Under a 0.1-MPa argon atmosphere, the values are expected to increase by an additional constant term of about 0.02 W/m/K. It showed that the thermal conductivity via the backbone of the carbon aerogel increases strongly with the pyrolysis or annealing temperature applied [86]; this is due to an increase in ordering of the carbon structure on the molecular scale accompanied by the growth of the carbonaceous microcrystallites. The study revealed that these structural changes mainly reduce the grain boundaries and thus the scattering of the phonons that dominate heat transport via the solid phase. In contrast, the electronic contribution to the thermal transport was

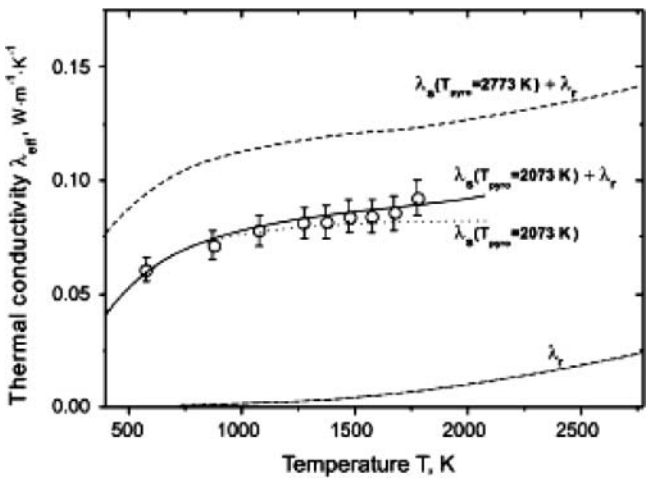

Figure 42. Thermal conductivities of a carbon aerogel [90].

shown to be negligible as would be expected for highly amorphous systems. Nevertheless, an earlier paper had already revealed the high potential of carbon aerogel as high-temperature thermal insulations [90].

In Figure 41, the thermal conductivity of the carbon aerogel (pyrolysis undertaken at 2073 K) under a 0.1-MPa argon atmosphere (filled circle) and vacuum (open circle) is shown as a function of temperature. Also shown is the thermal conductivity at 573 K of a carbon aerogel (prepared at a lower pyrolysis temperature of 1073 K) in 0.1-MPa argon atmosphere (filled triangle) and vacuum (open triangle) [90].

In Figure 42, the thermal conductivities of a carbon aerogel (prepared at a pyrolysis temperature = 2073 K) was measured as a function of temperature in vacuum (open circles); the radiative λ_r and solid λ_s contributions to the overall thermal conductivity are indicated and the full line represents the superposition of the two terms. The upper dashed line corresponds to the thermal conductivity expected for a similar aerogel, but pyrolysed at 2773 K [90].

2.7.2. LC-NCell aerogels

Nanocellulose, or nanofibrillated native cellulose, [87] has recently been attracting interest as a support structure for use in aerogels [88,91−96]. Cellulose is produced in plant tissues in the form of crystalline nanofibres with a width of approximately 3 nm. These nanofibres have a low density (1.6 g cm^3), a high strength (2−3 GPa), a high elastic modulus (110−140 GPa), and a large surface area (ca. 800 $m^{2/}g$); all of these properties render these nanofibres very suitable for aerogel skeletons [80, 97, 98] and the resulting nanocellulose aerogel is thus mechanically tough and flexible [81]. However, unlike silica aerogels, this type of aerogel does not show optical transparency and no linear elasticity and has a much lower surface area than expected. These unfavourable properties of the nanocellulose aerogel are related to their skeletal structures, which consist of randomly-connected, bundled nanofibres. Foam structures of nanocellulose and aerogels of regenerated cellulose prepared through molecular dissolution processes have also been described [82,99−102]. Aerogels that consist of three-dimensionally ordered nanofibre skeletons of liquid crystalline nanocellulose (LC-NCell; Figure 43) have also been reported. The LC-NCell used in that study was composed of surface-carboxylated cellulose nanofibres dispersed

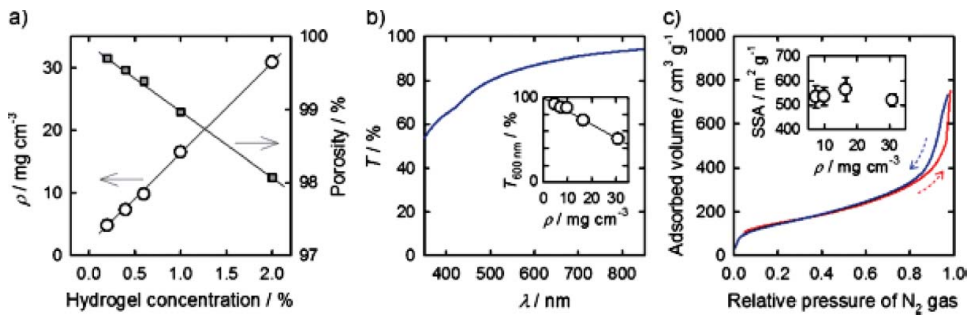

Figure 43. Structural characteristics of LC-NCell aerogel: (a) density and porosity of the aerogel as a function of hydrogel concentration; (b) light transmittance spectrum of the 1-mm-thick aerogel with a density of 10 mg cm^3 (inset: light transmittance at 600 nm as a function of density.); (c) nitrogen adsorption−desorption isotherm of the aerogel (inset: SSA of the aerogel estimated from the isotherms.) [146].

in water in a nematic LC order; it was prepared from wood cellulose by an oxidation reaction using 2,2,6,6-tetramethylpiperidine-1-oxyl as the catalyst [103–105]. The liquid crystalline arrangement of the nanofibres could be fixed using a dilute acid solution,[105] so that the fluid LC-NCell dispersions became stiff, free-standing hydrogels without volume shrinkage. A transparent LC-NCell aerogel was obtained by supercritical drying of these hydrogels. The ordered nanofibre network of the hydrogels was preserved in the aerogel even throughout the drying process. The structural properties of the LC-NCell aerogel could be easily regulated (Figure 43). The bulk densities (1) of the aerogel were found to increase in a linear manner with hydrogel concentration (Figure 43). The LC-NCell aerogels prepared in the study had very low densities (4–40 mg/cm^3; porosity: 98.1%–99.7%), and can therefore be categorized into the lowest density class of lightweight, porous materials. A low aerogel density results in a smaller dielectric constant and lower thermal conductivity. Upon drying of the hydrogels, the LC-NCell aerogel exhibited linear shrinkages of approximately 14%. These shrinkages were uniform for each side of the cube-shaped aerogel, suggesting that the LC-NCell aerogels were isotropic as bulk structures. In general, a linear shrinkage of 10%–15% is inevitable when supercritical drying is used to prepare an aerogel. Figure 43(b) shows the UV/Vis light transmittance spectrum of the LC-NCell aerogel. The 1-mm-thick LC-NCell aerogel, with a density of approximately 10 mg/cm^3, showed a high transmittance of 80%–90% in the visible light region, which decreased moderately in a linear manner with density (Figure 43(b)). This type of aerogel did not absorb in the visible light region; the LC-NCell aerogel is, therefore, colourless, as are silica aerogels. The blue appearance of the LC-NCell aerogel is caused by Rayleigh scattering of short-wavelength visible light by their thin skeletons. The nitrogen adsorption isotherms of the LC-NCell aerogel were characterized by hysteresis at a high relative pressure (Figure 43(c)). Such an isotherm is often observed for mesoporous structures with pore sizes of 2–50 nm [106]. The pores of the LC-NCell aerogel correspond to the spaces between the oriented nanofibres. The pore sizes of the LC-NCell aerogels as estimated from the isotherms ranged from a few nanometres to 100 nm, with a most probable value of approximately 30 nm with the increase in density (Figure 43). The SSAs of the LC-NCell aerogels were almost constant within a narrow range of 500–600 m^2/g (Figure 43(c)), indicating that the contact areas between the nanofibres remained constant even as the density was changed. From the SSA values, the nanofibre width of the aerogel skeleton could be estimated to be 4–5 nm, which is close to the width of isolated cellulose nanofibres (ca. 3 nm). A large SSA is important for the application of the aerogels as insulators, supports, and adsorbents [107].

In theory, the thermal conductivity of an aerogel in air is approximated by the sum of the heat transfer by the solid phase (skeleton; λ_{solid}), the gas phase (λ_{gas}), and radiation (λ_{rad}):

$$\lambda_{aerogel} = \lambda_{solid} + \lambda_{gas} + \lambda_{rad} \tag{2.21}$$

The contributions of the solid phase (λ_{solid}) and the gas phase (λ_{gas}) can be significantly reduced by lowering the bulk density of an aerogel and by narrowing the pore size to less than the mean free path of the gas molecules present in air (ca. 70 nm). The LC-NCell aerogel with the lowest conductivity displayed both a very low density of 17 mg/cm^3 and a characteristic pore size of approximately 30 nm (Figure 44), which should account for the

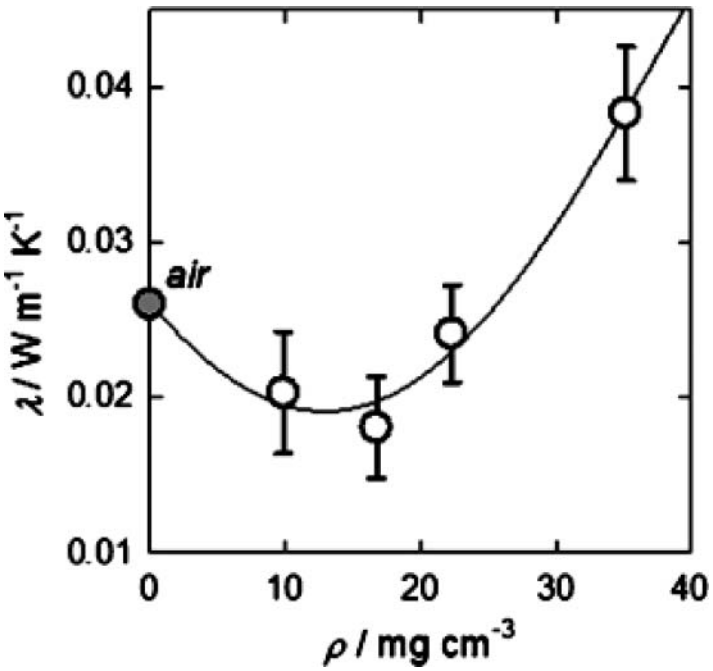

Figure 44. Thermal conductivity of LC-NCell aerogels as a function of density [146].

significant reduction in conductivity of this aerogel to a value that is smaller than the conductivity of air.

3. Applications of aerogels

Aerogel can be used for the development of a wide variety of novel high-performance products such as jackets for protection from extreme cold weather conditions, components in space suits, specialist building and pipeline insulation, acoustic and thermal insulation blankets, aerogel–textile composite materials, and many more (see Figure 45). Some of the main areas of applications of aerogel identified in the 1990s which include several areas involving textiles and still stand are

- interior and exterior insulating plasters for breathable building envelopes and facades;
- insulation boards for internal insulating finishing systems;
- industrial insulation;
- thermal insulation coatings for safe-to-touch surfaces, energy efficiency, prevention of corrosion under insulation (CUI), thermal breaks, and condensation control;
- insulation packs for oil and gas subsea pipelines;
- architectural daylighting panels, glass units, and tensile roofing systems;
- ultra-low-gloss matte paint coatings for industrial surfaces;
- non-wovens for architectural membrane roofing;
- outdoor gear and apparel;
- personal products including skin and beauty care.

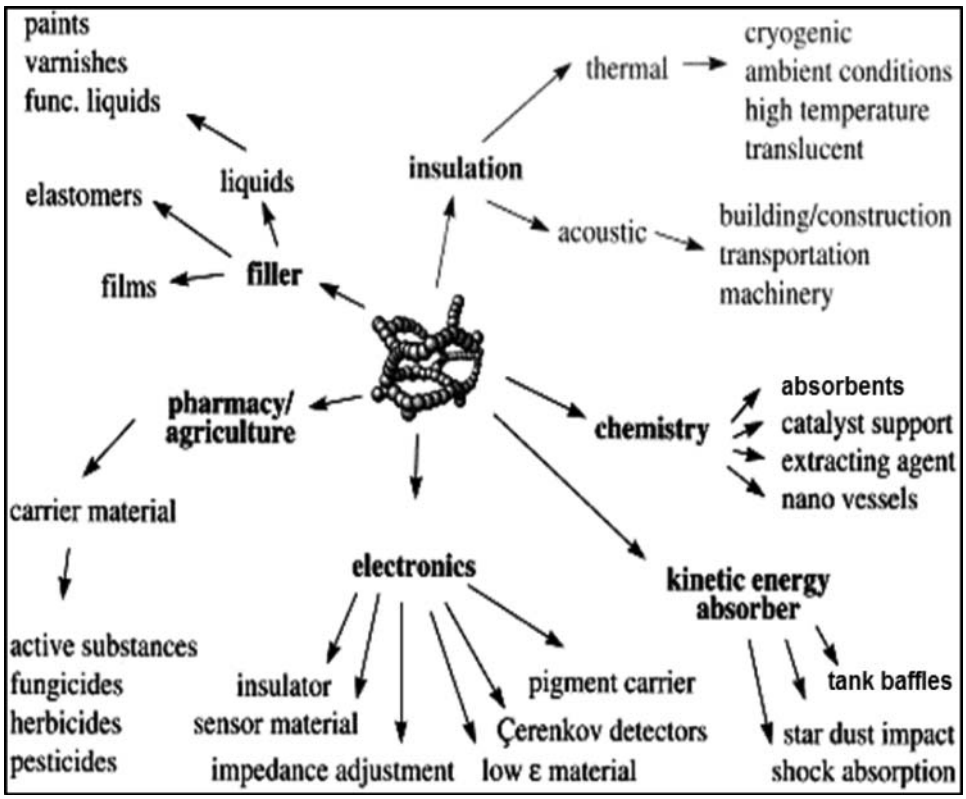

Figure 45. Applications of silica aerogel [18].

3.1. Aerogel blankets

Aerogel materials may also be applied to a building's walls, attics, grounds, and appliances. Aerogel blankets/panels have been developed to meet various demands, as shown in Figure 46, and commercial manufacture of aerogel blankets began around the year 2000 [108]. Aerogel blanket/panel is a composite of a silica aerogel and fibrous reinforcement that turns the brittle aerogel into a durable, flexible/solid and hydrophobic material, useful for building envelopes, inside or applications in buildings [108].

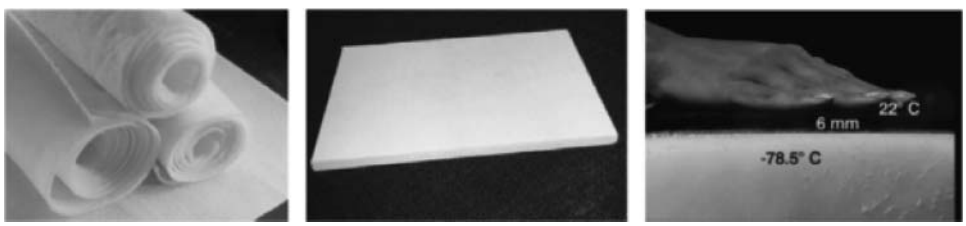

Figure 46. Flexible aerogel blankets and solid aerogel boards: (a) aerogel blankets [147], (b) aerogel panel [148], and (c) super-insulating aerogel blanket [147].

3.2. Housing, refrigerators, skylights, and windows

Silica aerogel can be synthesized using low-cost precursors at ambient pressure which makes aerogel suitable for commercialization. Aerogel transmits heat only one hundredth as well as normal-density glass. The first residential use of aerogel is as an insulator in the Georgia Institute of Technology's Solar Decathlon House, where it is used as an insulator in the semi-transparent roof. Aerogel is a more efficient, low-density form of insulation than the PUF currently used to insulate refrigerators, refrigerated vehicles, and containers, and it avoids the need to be blown into refrigerator walls, which used to be done by chlorofluorocarbon propellants, the chemical that has been one of the chief causes of the depletion of the earth's stratospheric ozone layer [109].

3.3. In clothing, apparel, and footwear

Aerogel blanket known as Spaceloft, which is used primarily in winter apparel products such as snowboard suits, is produced by trapping aerogel interstitially within a fibre matrix. To accomplish this, the matrix is impregnated with aerogel-forming precursor and supercritically dried under pressure. In 2002, Aspen Aerogel Inc. patented aerogel composite reinforced by a low-density fibrous batting in combination with one or both of short, randomly oriented microfibres and conductive layers. The aerogel composite material consists of two phases. The first is a low-density aerogel matrix and the second is a reinforcing phase. This reinforcing phase consists primarily of fibres, preferably a combination of the batting and one or more fibrous materials of significantly different thickness, length, and/or aspect ratio. A preferred combination of a two fibrous material system is produced when a short, high aspect ratio microfibre (one fibrous material) is dispersed throughout an aerogel matrix that penetrates a continuous lofty fibre batting (the second fibrous material). Such aerogel-based insulation materials can be used for insulation components in apparel and footwear applications.

Compared with traditional insulation materials for footwear and apparel applications that rely on textile, foam, or fibre technology, the insulating power of aerogel-based materials is found to be superior; they yield materials with a sub-nanoporous lattice structure that has a very high surface area and billions of irregularly shaped pores throughout the material. As a result, aerogels have from two to six times more insulating power than other commonly used materials. While all other materials rely on high thickness or loft to provide their insulation value, aerogels provide higher insulation values at greatly reduced loft. The difference between the temperature below and above the aerogel-insulated footwear is shown in Figure 47. For example, in order to maintain either stylish designs and/or functional performance in footwear applications, there is very little space available for insulation. The aerogel product Pyrogel® AR5401 (Aspen Aerogels Inc.), a carbon-filled aerogel, is claimed to be able to provide manufacturers with the ability to significantly upgrade the performance of their footwear and cold weather products, while increasing the freedom for design and the inclusion of other functional elements. Even under the minimal force of 1 PSI (6.89 kPa) applied in standard thermal testing, popular microfibre textiles can lose up to 75% of their thickness and insulating power, while aerogel maintains its original thickness. Compressive loads applied to footwear and apparel during use are significantly higher than 1 psi, but under loads of 15 psi, aerogels continue to retain over 95% of their thickness and 97% of their

Figure 47. Difference between the temperature below and above the aerogel-insulated footwear [149].

insulating ability [110], so they can be used to deliver consistently high insulating power [111]. The US company, Aerogels Inc., offers insulation components based on Aerotherm aerogel products for footwear as well as components for gloves and insulation panels for garments [112]. Aerogels can also be utilized in the development of novel anti-wetting coatings on textiles such as silica–biopolymer coating to render highly hydrophobic characteristics to the fabrics or to impart flame-retardant finishes to fabrics. A typical example is achieved by the coating of protective clothing with aerogels.

For applications where thermal conductivity must be minimized, heat transfer by the gas phase present in an aerogel could be avoided by evacuation. Evacuation of Si–aerogel reduces its thermal conductivity by 50%.

Commercial manufacture of aerogel 'blankets' began around the year 2000. Aerogel blanket is a composite of silica aerogel and fibrous reinforcement intended to convert brittle aerogel into a more useful product by incorporating it into a durable and flexible material. The mechanical and thermal properties of the product may be varied based upon the choice of reinforcing fibres, the aerogel matrix, and opacification additives included in the composite. Aspen Aerogel Inc. of Northborough, MA, for example, produces Spaceloft® as a relatively inexpensive and flexible blanket by incorporating a thin layer of aerogel embedded directly into the fabric; in promotional exercises, Mount Everest climbers have used aerogel insoles, as well as sleeping bags lined with the material [113].

3.4. Green buildings

Aerogel/fibre composites are available which aim to reduce the energy consumption in households and industries by providing higher levels of insulation from thinner sheets than those which would be required with traditional insulating batts such as those made from rockwool or fibreglass. The earliest form of insulation-incorporating aerogels was the aerogel blanket and this is still in widespread use. Studies have shown that aerogel blanket can reduce energy consumption from heating or cooling the interior of a fabric structure by 30%–70%, depending on the climate and is being used as

the insulation, for example, in sports stadia, recreational facilities, water parks, and 'green' shopping centres, and also in thermal awnings and blinds to provide a lower cost option to window replacement for retrofits of old buildings that must comply with new energy codes.

Some applications make use of more than one of the aerogel's characteristics. For example, a layered, tensioned textile composite roofing membrane called Tensotherm™, patented [113] and made by Birdair Inc., Amherst, NY, uses an aerogel-based insulation layer to trap air, prevent heat loss, and gain solar energy/daylight in the building by virtue of its ability to transmit and diffuse natural light. The Tensotherm™ composite membrane consists of three layers sandwiched together:

- a Polytetrafluoroethylene (PTFE)/fibreglass fabric exterior skin to provide durability, transparency, and protection from the elements;
- a layer of aerogel blanket to provide transparency and both thermal and acoustic insulations; and,
- a PTFE/fibreglass acoustic or vapour barrier interior liner.

4. Global necessity of super-insulation

The first global oil crisis in 1970s dramatically affected the whole world and clearly showed the growing dependence of modern society on imported oil and vital need for cheap, renewable, and environmentally friendly energy technologies. Due to the limited supply of fossil fuels and growing significance of environmental issues, developed countries needed to check their energy strategies and politics. There was, and still is, also a crucial need to stabilize the CO_2 concentration in the atmosphere and then to reduce it to minimize its effects on the global climate. Stabilization of atmospheric CO_2 concentration below 500 ppm is regarded as the first step [114]. That was a significant move but very difficult to implement in a short period because of the huge dependence of modern society on oil, gas, and coal. Moreover, replacing fossil-fuel-based applications with renewable energy technologies all over the world includes some severe technological difficulties and economic barriers. Nevertheless, short-term, medium-term, and long-term strategies were developed to narrow the gap between fossil fuels and renewable energy systems. Appropriate strategies for halting global climate change were sorted by time and source, and the target steps were divided into three groups headed mobility, power plants/heavy industry, and, finally, buildings as illustrated in Table 10. The results (perhaps surprisingly) indicated that building sector plays a remarkable role in global energy consumption, taking a larger share, for example, than that of the mobility sector. It was also noted that HVAC (heating, ventilation, and air conditioning) accounts for the lion's share of energy consumption by buildings. This situation highlighted the necessity for more stringent thermal insulation standards for buildings, to levels which can be described as super-insulation [115]; super-insulating glazing and aerogel blankets are becoming more widely available in the insulation market [116].

Any thermal insulation material aims to reduce heat loss, and so a low thermal conductivity or high *R*-value is of prime importance. A high *R*-value means that a thinner layer of insulation can be used, leading to a smaller space requirement; for example, according to its product data sheet, a 10 mm thickness of Thermablok™ fibre-

Table 10. Short-, medium-, and long-term strategies for halting global climate change [150].

Short-term	Medium-term	Long-term
Mobility		
Increasing drive efficiency, hybrid systems, weight reduction	Only electrical and hybrid vehicles are available on markets	Short-range fuel-cell and hydrogen-technology-powered mobility picks up; fossil fuels reserved for long-range mobility
Power plants/heavy industry		
Establishing possibilities for CO_2 sequestering; slight increase in number of nuclear plants to provide more of the steady, continuously required level of energy and other intermittent systems to deal with peaks	Sequestration implemented growing contributions of renewables (sun, wind, water), improved electrical storage	All plants operate nearly CO_2 free, renewables dominate the mix, nuclear and fossil-fuelled plants are only for volume support; robust grid and storage systems are in place
Buildings		
Reducing energy demand of HVAC by thermal insulation, developing zero-energy buildings	New buildings are CO_2 neutral, wide use of photovoltaics; retrofitting of old buildings required by law	More than 50% of all buildings are no longer net producers of CO_2; retrofitting of all buildings continues; buildings store notable amounts of electricity

reinforced laminated insulation blanket (Thermablok Aerogels Ltd, Ashford, Kent, UK) is quoted as providing an *R*-value of 0.769 (m^2/KW), around twice that of the best competitor insulating material [117]. Omer et al. [118] evaluated various insulation materials and compared their thermal conductivities; aerogel showed the lowest thermal conductivity, and its manufacturing cost has the potential to be reduced drastically, if it is produced in a rapid single-step process using ambient drying.

4.1. Advantages and limitations

4.1.1. Advantages of aerogels

Aerogel is regarded as one of the most promising high-performance thermal insulation materials for building applications today. With a low thermal conductivity (~13 mW/mK), it shows remarkable characteristics compared to traditional thermal insulation materials. Also higher transmittances in the solar spectrum are of great interest for the construction sector; their visible transparency for insulation applications allows their use in windows and skylights which give architects and engineers the opportunity of reinventing architectural solutions, a prospect which has now been put into practice [115] in an insulated tensile fabric roofing material. Also, the low thermal conductivity, a high solar energy, and daylight transmittance in monolithic silica aerogel make it a very interesting material for use in highly energy-efficient windows [119]. For cryogenic systems, multilayered insulation (MLI) is the insulation of choice. However, MLI requires a high vacuum for optimal effectiveness, whereas powder insulations such as glass microspheres and aerogel beads have shown promise at soft vacuums and have a structural advantage in that they are far simpler to install and maintain [118, 120–123].

Due to its porous structure and low density, aerogel can trap dust-sized space projectiles travelling with hypervelocity speed; NASA, therefore, used aerogels to trap space dust particles and for the thermal insulation of space suits [124–126].

Indoor environments can become polluted by the chlorine from tap water, volatile organic compounds from organic solvents, formaldehyde from furniture and paints, SO_2 and NO_2 from the incomplete combustion of gases in heating and cooking appliances and a range of hydrocarbons. Airborne contaminants are associated with respiratory problems and allergies like asthma; their conversion into nontoxic compounds is an effective pathway for their removal and for protecting the environment; modified aerogels offer a solution for removal of airborne contaminants [127]; they have the potential to be more environmentally friendly than systems involving the use of noble metal catalysts due to the negative environmental impact associated with mining and processing the metals involved [128]. Modification of the aerogel is essential to achieve specific functionality and this tailoring can start during the sol−gel process either following gelation or after obtaining the aerogel. Suitable modification can be achieved via either

(1) surface functionalization of aerogel for regulating the adsorption capacity, or
(2) applying a polymeric coating on aerogel surface. Hybrid aerogel materials can encompass the intrinsic properties of aerogels (high porosity and surface area) with the mechanical properties of inorganic components and the functionality and biodegradability of biopolymers [129−131].

4.1.2. Limitations of aerogels

Widespread uses of aerogel materials are restricted at present mainly due to high production costs, poor mechanical properties, and health issues associated with the release of fine particles if crushed. The main issues are their mechanical brittleness (unless supported/protected by reinforcement materials or covered by a membrane) and the energy-consuming and time-consuming fabrication process, which requires long periods of temperature-controlled ageing, solvent exchange, and supercritical drying.

To overcome the mechanical brittleness of aerogels which is intrinsic to their skeletal structure and limits their applications, the hybridization of aerogels with organic polymers is considered to be a fruitful approach [132−137]; reinforcement introduces significant decreases in porosity and surface area.

Supercritical drying is the most expensive and risky step in the process of making an aerogel. A highly desirable goal in aerogel preparation was the elimination of the supercritical drying process and there has been some success. For example, Guo and Guadalupe [134] succeeded in synthesizing a silica-based aerogel from a metastable lamellar composite through cooperative interaction between silica and surfactant species [138]. The surfactant molecules used to generate pores were able to be removed from the silica network through conventional solvent extraction and no supercritical extraction was necessary [139].

Although silica aerogels are very fragile, the strength of silica aerogel monoliths has been improved by a factor of >100 times by cross-linking the nanoparticle building blocks of preformed silica hydrogels with polyhexamethylene diisocyanate. These composite monoliths are much less hygroscopic than native silica, and they do not collapse when in contact with liquids [140].

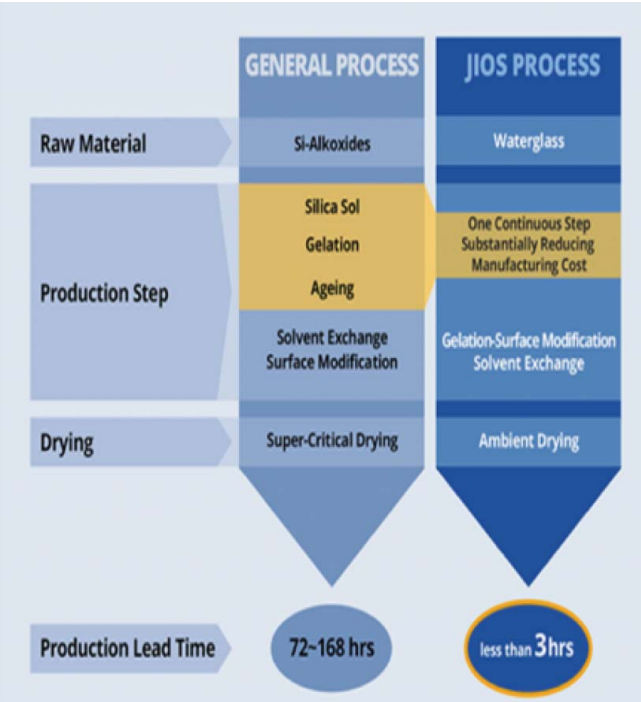

Figure 48. JIOS one-step continuous process.

Aerogel is a mechanical irritant to the eyes, skin, respiratory tract, and digestive system. Small aerogel particles can potentially cause silicosis, and so forth, when inhaled and can induce dryness of the skin, eyes, and mucous membranes. Therefore, protective gear including respiratory protection, gloves, and eye goggles must be worn while handling aerogel [141]. Products are now available, however, which are safe to touch and/or encapsulated to enable them to be worked [138].

4.1.3. Development of low-cost aerogels by a one-step continuous process

The company JIOS was founded by project leaders in a Korean government-sponsored research team that developed new approaches to the production of silica aerogel. Since its founding in 2010, JIOS has continued to invest heavily in R&D and engineering to be able to produce aerogel at rapidly declining costs. They sell high volumes of powder directly to top-tier industry partners. Until the founding of JIOS, high costs and low volumes had prevented the mass development of aerogel for everyday applications. JIOS uses a novel, proprietary production process that employs readily-available raw materials, a one-step continuous process which combines sol−gel, gelation, and ageing, and an ambient drying process all of which help to reduce the production cost. JIOS' ambient drying process differs substantially from the standard 'supercritical drying' process and drives production time down from the usual several days to less than 3 hours. JIOS' disruptive pricing is considered to offer global

Table 11. Comparison of performance and cost of different thermal insulating materials [138].

Material	Thermal conductivity (W/m K)	Minimum improvement (= reduction) in conductivity over brick or stone	Indicative costs
Brick or stone	0.6–2.5	-	
Natural insulation materials	0.03–0.05	20	£9–£18/m^2
Mineral insulation	0.03–0.04	20	£5/m^2
Petrochemical insulation	0.02–0.04	30	£5–£22/m^2
Layered foil	0.033–0.035	18	£8–£9/m^2
Aerogel	0.013–0.014	42	£20–£30/m^2
Vacuum-insulated panels	0.004–0.01	60	£40–£50/m^2

manufacturing leaders the opportunity to develop aerogel-enhanced performance lines at market-acceptable prices.

To help customers bring their aerogel-enhanced products to market faster and with less risk, JIOS has also developed aerogel application technologies and intellectual property in target industries which are licensed and shared with customers including, for example, Etex Group, a Belgian company supplying building products.

4.2. Comparative performance and cost

Natural-fibre-based thermal insulation materials perform at least 10 times better than brick or stone (see Table 11). Newer insulation materials perform at least 20 times better than brick or stone, and aerogels over 40 times better, while vacuum-insulated panels are better still, at least 60 times better than brick or stone. However, both aerogels (the best performing new insulation material), and vacuum-insulated panels, remain very expensive. Table 11 shows a comparison of performance and cost of different thermal insulating materials [138]. Figure 48 shows a comparison of insulation properties of aerogel against other materials.

4.3. Commercial manufacturers and products

During the last five years, large-scale commercial production of nanoporous aerogel materials has been achieved. The financial motivation for this business development was due, in large part, to the potential applications in thermal insulation. Comparison of characteristics of different kinds of insulation is shown in Table 12. For example, products now available include aerogel non-woven sheet for cold-weather applications manufactured by Cabot Corporation [142], aerogel composite blankets manufactured by Aspen Aerogel, Inc. [140], and aerogel insoles manufactured by Aerotherm. Minimum and maximum conductivity of some insulation materials are shown in Figure 49. Because they are fully breathable and hydrophobic, these materials are ideal candidates for thermal insulators in a variety of applications. As illustrated in Table 13, there are currently 16 major companies which are involved in the production of different types of aerogel. They either use aerogel for the production of their own products or they distribute and supply to other industries. The data have been collated from Boston Business Journal/Business Week (http://www.maerotech.com/prospect3.html) company websites.

Table 12. Comparison of characteristics of different kinds of insulation [138].

	Natural/cellulose insulation	Mineral insulation	Petrochemical insulation	Layered foil	Vacuum-insulated panels	Gas-filled panels	Aerogel
Conductivity (mW/mK)	40–50 (cork) 40–50 (cellulose) 39 sheep wool	30–40	30–40 expanded polystyrene, 20–20 polyurethane	33–35	4–10	40 typical	13–14 commercial
Breathable	Yes	Yes	Variable (may have facing)	No	No	No	Yes
Absorbs moisture	Yes and moisture will reduce insulation	Yes but not so much as with cellulose	Variable	No	No	No	Usually hydrophobic to reduce condensation
Can be cut to fit	Yes	Yes	Yes	Yes	No	No	Yes
Installation considerations	Must be ventilated	Some fibres can cause lung damage (risk to workers	Joints between panels must be sealed	None	Very delicate – best suited to prefabricated component	As VIPs but not so bad	Cutting raises dust but not expected to be a health risk. Fragile in tension
In-use considerations	Must be ventilated to prevent mould and fungus	None	Toxic fumes can be released in case of fire	None	Easily damaged. Expected age varies, even without a puncture	As VIPs but not quite so bas as not undue vacuum	
Scalable	Yes	Yes	Yes	Yes	Manufacturing complex with manual steps	Yes	Yes
Maturity	Product	Product	Product	Product	Product	Development abandoned	Early products

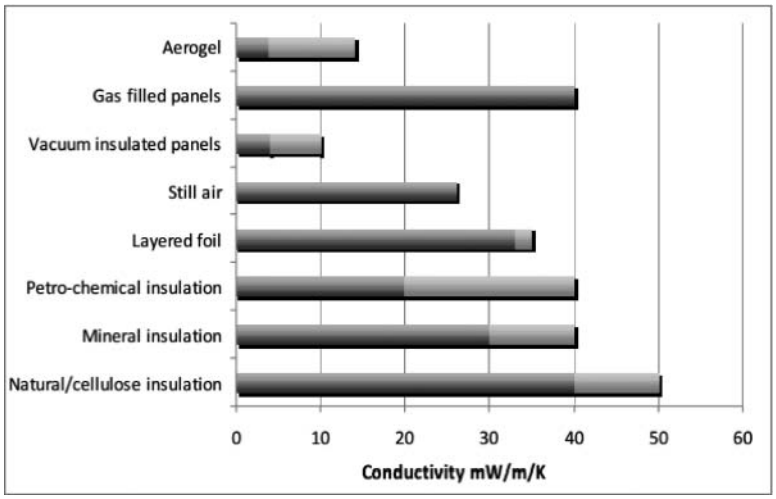

Figure 49. Minimum and maximum conductivity of some insulation materials [138].

Table 13. Global aerogel industry players by alphabetical order.

No	Company	Activities	Annual revenue*	Base
1	Active Aerogels	Nanostructured materials for thermal insulation and for adsorption of pollutants, applicable in aerospace, oil and gas industries, housing, and wastewater treatment.	N/A	Portugal
2	Aerogel Composite Inc.	Develop and supply aerogel-based composite materials for a wide variety of industries, e.g. a carbon aerogel based electrocatalyst for use in the manufacturing of fuel cell electrodes to reduce the platinum requirements for fuel cell vehicles.	$1-10 mil	USA
3	Aerogel Technologies LLC	Airloy Ultramaterials; super-insulating with machinability, durability, and strength in the form of aerogel discs, blocks, tiles, particles, and super-insulating blankets	N/A	USA
4	Airglass	Monolithic aerogel (blocks and tiles), blankets, granular, powder, coatings, etc.	N/A	Sweden
5	American Aerogel Corporation	Insulated packaging for superior temperature protection against both high and low ambient temperatures,	$1—10 mil	USA
6	Aspen Aerogel Inc.	Pyrogel® XT-E high-performance insulation material for the industrial market. Cryogel® Z cryogenic insulation is used in below-ambient temperature applications in the oil and gas processing industry and industrial appliances.	$3.8 mil	USA
7	BASF SE	Insulating material with insulation values of 16 mW/mK compared to those of 21—40 mW/mK for classical insulating materials. The material, SLENTITE™, is a polyurethane aerogel with 50—100 nm pores.	N/A	Germany
8	Cabot Corporation	High-quality particulate silica aerogel solutions for energy-efficient buildings and industrial infrastructure, safe-to-touch surfaces, personal care products, interior and exterior insulating plasters, industrial insulation, outdoor gear and apparel	$2.1 bil	USA

(*continued*)

Table 13. (*Continued*)

No	Company	Activities	Annual revenue*	Base
9	CDT Systems Inc.	In excess of 3 volts, carbon aerogel electrodes perform electrolysis, or the separation of a hydrogen/oxygen mix from water for improved fuel economy and reduced harmful emissions.	$32 k	USA
10	CF Technologies	Custom formulation for high-performance thermal and acoustic insulation, multi-component catalysts, adsorbents, and ceramic precursors, monolithic custom-made aerogels, supercritical drying laboratory and pilot scale services	$750 k	USA
11	Cooper Electronic Technologies Inc.	PowerStor Aerogel Capacitors, ultra-high capacitance devices based on carbon aerogel.	$17.5 bil	USA
12	Dow Corning Corporation	White free-flowing 100% hydrophobic aerogel powder for use in hair care, skincare, fragrance delivery, and antiperspirants/deodorants.	$4.9 bil	USA
13	Enersens SAS	Aerogels and insulators for the construction and industrial sector. Its products include granules, silica aerogel, panels, and matelasses.	N/A	France
14	Guangdong Alison Hi-Tech Co. Ltd.	Alison Aerogel Blanket DRT06 Series is a series of flexible high-temperature insulation blankets in which silica aerogel is composited with fibres.	N/A	China
15	Honeywell International Inc.	Aerogel bases mould for MEMS fabrication and formation, a patterned aerogel-based layer that serves as a mould for at least part of a microelectromechanical feature.	$34.6 bil	USA
16	JIOS Aerogel Corporation	JIOS employs a one continuous step process which combines sol-gel, gelation, and ageing, and an ambient drying process to reduce production cost. JIOS' ambient drying process differs from the standard 'supercritical drying' process and drives production time down from the usual several days to less than 3 h.	N/A	South Korea
17	Marketech International Inc.	Marketech offers a line of standard silica, organic and carbon aerogels that include monoliths, ingots, random pieces, powders, and composite papers.	$1.8 mil	USA
18	Matsushita (Panasonic) Electric Works	Employs a waterproofing process to lengthen the lifetime and optical efficiency of silica aerogel for a variety of applications, including the cladding and protection of optical fibre.	$12.9 bil	Japan
19	Nano High-Tech Co. Ltd.	Aerogel, aerogel blanket, aerogel insulation felts manufacturer/supplier based in China, offering 3, 6, and 10 mm aerogel blanket for wall insulation, tanks and pipes insulation, flexible jackets, etc.	N/A	China
20	NanoPore Inc.	NanoPore™ thermal insulation for both vacuum insulation and ambient pressure applications. NANOGLASS© is a family of inorganic porous oxide-like low-*k* dielectric materials suitable for applications requiring ultra-low-*k* values. NanoCool™ is for maintaining product temperature during shipment without the need to use frozen cool packs.	$1.8 mil	USA
21	Ocellus Technologies	Nanoporous foams (nanofoams) and aerogels including nanofoam materials made from silica, alumina, phenolic resins, and carbon for aerospace and industrial applications.	N/A	USA
22	TAASI	Aerogel products in a powder form for general packaging, food, pharmacological and laboratory packaging and the Pristina™ personal air filter	$750 k	USA
23	United Nuclear Scientific Equipment & Suppliers	Monolithic aerogel from silica, in the form of thermal blankets, powder, etc.	N/A	USA

Note: *Revenue figures may include income generated by other products and operations.

5. Conclusion

Compared to other insulation materials, aerogel-based materials have considerably lower thermal conductivity and higher thermal resistance even at extreme temperatures, characteristics which are attributable to their low sample density; the aerogel component in aerogel blankets, for example, has a significant effect on its thermal properties. Whilst the thermal resistance (Rct) of the aerogel blanket fabric shows an increase as the fabric thickness increases in some applications, only a very thin sheet is required to achieve the desired degree of insulation. Such products are beginning to emerge and point the way towards the achievement of higher performance fabrics in terms of thermal insulation. Moreover, thermal measurements show that embedding silica aerogel in nanofibrous layers leads to increased thermal insulation, so performance gains in existing thermal insulation materials may be possible by incorporating a proportion of nanofibres into the structure, but large-diameter fibres would still be necessary for durability and compression recovery.

Carbon and other types of aerogel are effective absorbers of IR radiation and, in some cases, actually increase the mechanical strength of the aerogel. At ambient pressure the addition of carbon lowers the thermal conductivity from 0.017 to 0.0135 W/mK. In the case of cold weather clothing, higher thermal resistance is very important. This may be attributed to decrease in heat losses due to insulation by nano-airspaces inside aerogel present in the fabric. To fully realize the potential of aerogel, continued efforts are required to tackle the outstanding technical issues and improve the practical feasibility of the aerogel fabrication. Until recently, the batchwise step-by-step preparation of aerogels completed by supercritical drying was considered to be both essential and the most effective process, but it takes considerable time to complete and the final supercritical drying step adds considerable expense to the manufacturing process. However, significant progress has been made and recently JIOS, a producer of aerogel powder established in 2010 in South Korea, has developed methods for producing aerogels more rapidly and at lower prices by adopting a single-step continuous production process and ambient drying. With potential applications in films and threads, one of the company's primary target industries is textiles.

In the past, aerogels were dismissed for use in clothing as those made from silica can be fragile and brittle. Various approaches have been taken to overcome such disadvantages. For example, in 2012, researchers at NASA reported that altering the composition and structure of an aerogel by using polymers to reinforce the networks of silica could make it highly flexible and up to 500 times stronger. Another similar but separate method reported was to reinforce polyimide with brace-like cross-links to further strengthen the aerogel; such products could be produced in the form of a thin film sufficiently flexible to be used in highly insulating clothing that is less bulky than traditional 'thermal' garments, in spacesuits and firefighters' protective gear. Aspen Aerogels recommend incorporating Spaceloft™ aerogel blanket in insulating apparel and the fibre-reinforced, carbon-filled Pyrogel® in footwear. In yet another approach utilizing existing aerogel materials, adopted by Aerogel Technologies, encapsulated aerogel blanket is prepared and sold in sets suitable for use as panels in clothing or footwear; the accent is on the elimination of dust during cut-and-sew or similar clothing manufacturing methods; these products are already on the market under the name of Aerotherm.

5.1. Future direction

Analysts forecast the global aerogel market to grow at a CAGR of 35.86% over the period 2014–2019. The high number of patents being filed for new uses of aerogel and the development of new aerogel-based products is expected to contribute to market growth in the coming years [126]. However, to improve development opportunities and to take full advantage of aerogels' excellent thermal insulating abilities, further research needs to be conducted in the areas of

- synthesis and characterization of various types of aerogel focused on high-performance textiles;
- manufacturing methods for further process improvement and cost reduction to add to those already making an impact such as JIOS's rapid one-step and ambient drying process;
- new types of aerogel composites with properties desirable in clothing and footwear;
- development of new methods to treat fabrics with aerogel particles to reduce fragility and sensitivity to moisture;
- refinement of thermal measurement techniques as the existing measurements are designed mostly for standard ambient conditions and are not suitable for high-performance insulation materials at extreme temperatures;
- fabrication of new devices for the measurement of thermal properties in fibrous structures;
- modelling of convective heat transfer phenomena in fabrics treated with aerogels to enable better understanding of the thermodynamics under extreme temperature conditions;
- develop or update standards for thermal measurement in aerogel-based insulation materials used for textile applications, because existing standards do not address the necessary parameters under extreme conditions.

Funding

The authors gratefully acknowledge the support by Czech-India project [grant number: DEBEL-19027] and project No. L1213 of program NPU in Czech Republic.

Disclosure statement

No potential conflict of interest was reported by the authors.

References

[1] A. Taher, *Scientists Hail 'Frozen Smoke' as Material that Will Change World*, Sunday Times, *Timesonline*, 19 August 2007.
[2] S.S. Kistler, J. Phys. Chem. 39 (1) (1935) p.79.
[3] K. Higa, Illumin 14 (3) (2014) p.1.
[4] A.D. McNaught and A. Wilkinson, *Compendium of Chemical Terminology, IUPAC Goldbook, PAC*, 2nd ed., Blackwell Science, Cambridge, 2007.
[5] M.A. Aegerter, N. Leventis and M.M. Koebel, *Aerogel Handbook.* Springer, New York, 2011.
[6] http://www.reportlinker.com/p0118043-summary/Aerogels-BCC-Research.html

[7] http://www.designingbuildings.co.uk/wiki/Aerogel_market
[8] A.C. Pierre and G.M. Pajonk, Chem. Rev. 102 (2002) p.4243.
[9] G. Reichenauer and Z. Bayern, *In Kirk-Othmer Encyclopedia of Chemical Technology*. Wiley, New York, 2008.
[10] N. Husing and U. Schubert, Angew. Chem. Int. Ed. 37 (1–2) (1998) p.22.
[11] S.S. Kistler, Nature 127 (3211) (1931) p.741.
[12] D.M. Smith, R. Deshpande and C.J. Brinker, Ceramic Trans. 31 (1993) p.71.
[13] S.T. Mayer, R.W. Pekala and J.L. Kaschmitter, J. Electrochem. Soc. 140 (2) (1993) p.446.
[14] N. Leventis, N. Chandrasekaran, C. Sotiriou-Leventis and A. Mumtaz, J. Mater. Chem. 19 (1) (2009) p.63.
[15] B.C. Tappan, M.H. Huynh and M.A. Hiskey, J. Am. Chem. Soc. 128 (20) (2006) p.6589.
[16] K. Richter, P.M. Norris and C.L. Chang, *Aerogels: Applications, structure and heat transfer phenomena*, in *Review on Heat Transfer*, K.V. Prasad, Y. Jaluria and G. Chen, eds., Begell House Publishers, Danbury, CT, 1995. p.61.
[17] L.W. Hrubesh, J. Non-Crystalline Solids 225 (1-3) (1998) p.335.
[18] M. Schmidt and F. Schwertfeger, J. Non-Crystalline Solids 225 (1–3) (1998) p.364.
[19] *The Annual Review of Heat Transfer*, Vol. 14, University of Iowa, 2005.
[20] http://www.patentinsightpro.com/techreports/0610/Technology%20Insight%20Report-Aerogels.pdf
[21] http://45nrth.com/products/gloves/sturmfist-5
[22] https://www.shivershield.com/faqs/
[23] http://www.aerotherminsulation.com/products-applications/universal-insulation-panels-apparel
[24] http://aerotherminsulation.com/sites/default/files/Aerotherm%20Tech%20Datasheet%202012.pdf
[25] Z. Qi, D. Huang, S. He, H. Yang, Y. Hu, L. Li and H. Zhang, J. Eng. Fibers Fabrics 8 (2) (2013) p.134.
[26] A. Shaid, M. Furgusson and L. Wang, Chem. Mater. Eng. 2 (2) (2014) p.7
[27] M. Ayers, *At Elevated Pressures: The Life and Science of Samuel S. Kistler*, Ernest Orlando Lawrence Berkeley Laboratory, Berkeley, CA, 2000.
[28] M.A. Ayers and A. Hunt, *A Brief History of Silica Aerogels*. Ernest Orlando Lawrence Berkeley Laboratory, Berkeley, CA, 1996.
[29] *Aerogels: Their History, Structure, and Applications*. Copyright 2001 by George Beckingham. Available at http://geobeck.tripod.com/frontier/aerogels.html#link
[30] *Thermal Properties of Silica Aerogels*, Ernest Orlando Lawrence Berkeley Laboratory, Berkeley, CA, 1996.
[31] J. Cai, S. Lucas, L. Wang and Y. Cao, Adv. Mater. Res., 391–392 (2012) p. 116.
[32]. B. Xu, J.Y. Cai, N. Finn and Z. Cai, Micropor. Mesopor. Mater. 148 (1) (2012) p.145.
[33] B. Xu, J.Y. Cai, Z. Xie, L. Wang, I. Burgar, N. Finn, Z. Cai and L. Wong, Micropor. Mesopor. Mater. 148 (1) (2012) p.152.
[34] Y.C. Kwon, J. Civil Eng. Arch. 7 (12) (2013) p.1494.
[35] A. Du, B. Zhou, Z. Zhang and J. Shen, Materials 6 (3) (2013) p.941.
[36] Uzma-Parveen Khwaja-Husain Bangi, *Preparation and characterization of hydrophobic aerogels using inorganic precursor by ambient pressure drying*, PhD Thesis, Shivaji University, India, 2012, p.149–155.
[37] J. Fricke, E. Hummer, H.J. Morper and P. Scheuerpflug, Revue De Physique Appliquee Colloque C4, Supplement au n4, Tome 24, Avril 1989.
[38] B. Xu, J.Y. Cai, N. Finn and Z. Cai, Micropor. Mesopor. Mater. 148 (1) (2012) p.152.
[39] A.V. Rao, S.D. Bhagat, H. Hirashima and G.M. Pajonk, J. Colloid Interface Sci. 300 (1) (2006) p.279.
[40] S. Brunold, R. Frey and U. Frei, Proc. SPIE 2255 (1994) p.107.
[41] R.P. Patel, N.S. Purohit and A.M. Suthar, Int. J. Chem. Tech. Res. 1 (4) (2009) p.1052.
[42] B. Hosticka, P.M. Norris, J.S. Brenizer and C.E. Daitch, J. Non-Crystalline Solids. 225 (1) (1998) p.293–297.

[43] C. Moreno-Castilla and F.J. Maldonado-Ĥodar, Carbon 43 (3) (2005) p.455.
[44] M.B. Bryning, D.E. Milkie, M.F. Islam, L.A. Hough, J.M. Kikkawa, and A.G. Yodh, Adv. Mat. Res. J. 19 (5) (2007) p.661.
[45] Y. Tao, M. Endo and K. Kaneko, Recent Patents Chem. Eng. 1 (2008) p.192.
[46] M.-L. Liu, D.-A. Yang, and Y.-F. Qu, J. Exp. Nanosci. 5 (1) (2010) p.83.
[47] Y. Guo, H. Wang and L. Zeng, J. Non-Crystalline Solids. 428 (2015) p.1.
[48] J. Wang, Y. Zhang, Y. Wei and X. Zhang, Micropor. Mesopor. Mater. 218 (2015) p.192.
[49] A. Pons, L. Casas, E. Estop, E. Molins, K.D.M. Harris and M. Xu, J. Non-Crystalline Solids. 358 (3) (2015).
[50] W. Dong, J.S. Sakamoto and B. Dunn, Sci. Technol. Adv. Mater. 4 (1) (2003) p.3.
[51] G. Pajonk, E. Elaloui, R. Begag, M. Durant, B. Chevalier, J.-L. Chevalier and P. Achard, Process for the preparation of monolithic silica aerogels, US Patent No. 5795557 A, Universite Claude Bernard, Produits Chimiques Auxiliares, Armienes, Centre Scientifique Et Technique Du Batiment, 1996.
[52] H. Tamon, T. Kitamura and M.O. Kazaki, J. Colloid Interface Sci. 197 (2) (1998) p.353.
[53] D.M. Smith, A. Maskara and U. Boes, J. Non-Crystalline Solids 225 (1−3) (1998) p.254.
[54] A. Soleimani Dorcheh and M.H. Abbasi, J. Mater. Proc. Technol. 199 (1) (2008) p.10.
[55] V. Prevolnik, P.K. Zrim and T. Rijavec, Contemp. Mater. 1 (5) (2014) p.117.
[56] *Thermal Conductivity of Some Common Materials and Gases Web Site* (2012). Available at http://www.engineeringtoolbox.com/thermal-conductivity-d_429.html.
[57] *Aspen Aerogel Web Site* (2012). Available at http://www.aerogel.com/
[58] W.J. Platzer, *Optical Measurement of Granular Aerogel*, Frauenhofer Institute for Solar Energy Systems, Internal Paper, Ingenieurbuero Ortjohann, Freiburg im Breisgau, Germany, 1998.
[59] M. Reim, *Optische und thermische Charakterisierung einer mit Aerogel gefuellten Verglasung*, Report ZAE 2 −0700 − 5 2000, Bavarian Center for Applied Energy Research, Erlangen, 2000.
[60] N.C. Shukla, A. Fallahi and J. Kosny, in *Building Enclosure Science & Technology (BEST3) Conference*, 2012, Atlanta.
[61] M. Abu Shaid, Chem. Mater. Eng. 2 (2) (2014) p.37.
[62] M.L. Nuckols, D. Hyde, J.L. Wood-Putnam, J. Giblo, G.J. Caggiano, J.A. Henkener and B. Stinton, *Diving for science*, in Proceedings of the American Academy of Underwater Sciences 28th Symposium, N.W. Pollock, ed., AAUS, Dauphin Island, AL, 2009.
[63] H. Wu, Y. Chen, Q. Chen, Y. Ding, X. Zhou, and H. Gao, J. Nanomater. (2013) p.8.
[64] Z. Deng, J. Wang, A. Wu, J. Shen and B. Zhou, J. Non-Crystalline Solids 225 (1998) p.101.
[65] *Aerogel Web Site* (2012). Available at http://www.aerogel.com/products/pdf/Pyrogel_XT_DS.pdf
[66] D. Frank and A. Zimmermann, Aerogel composites, process for producing the same and their use, US Patent number: 5789075, 1998.
[67] A. Venkateswara Rao, *Aerogel handbook*, Springer, New York, 2011.
[68] T. Filetin, *Primjena nanomaterijala u tehnici* [*Application of Nanomaterials in Engineering*]. Available at http://titan.fsb.hr/~tfiletin/pdf/hazu_nano1.pdf
[69] *Thermal Conductivity of Some Common Materials and Gases Web Site* (2012). Available at http://www.engineeringtoolbox.com/thermal-conductivity-d_429.html
[70] K.T. Regner, et al. Nat. Commun. 4 (1640) (2013) doi:10.1038/ncomms2630.
[71] G. Chen, Int. J. Thermal Sci. 39 (2000) p.471.
[72] *Aspen Aerogels*. Available at http://www.airtightdistribution.com/pdfs/Spaceloft_Brochure.pdf.
[73] SDL, *Instruction Manual for the m259b Sweating Guarded Hot Plate*. SDL ATLAS Textile Testing Solutions, Stockport, 2011.
[74] J. Fresnais, J.P. Chapel and F. Poncin-Epaillard, Surf. Coatings Technol. (2006) p.5296.
[75] J. Huang, Polym. Testing 25 (5) (2006) p.709.
[76] S. Henning and L. Svensson, J. Non-Crystalline Solids 23 (1981) p.697.
[77] A.S. Dorcheh and M.H. Abbasi, J. Mater. Proc. Technol. 199 (1−3) (2008) p.10.
[78] M. Schmidt and F. Schwertfeger, J. Non-Crystalline Solids 225 (1998) p.364.

[79] H. Zhang, C. Hong and Y. Qiao, *Synthesis, Structural and Thermal Properties of Nano-porous SiO_2-based Aerogels*. Available at http://cdn.intechopen.com/pdfs/15399/InTech-Synthesis_structural_and_thermal_properties_of_nano_porous_sio2_based_aerogels.pdf
[80] M. Wiener, G. Reichenauer, F. Hemberger and H.-P. Ebert, Int. J. Thermophys. 27 (6) (2006) p.1826.
[81] R.T. Olsson, M.A.S.A. Samir, G. Salazar-Alvarez, L. Belova, V. Strçm, L.A. Berglund, O. Ikkala, J. Nogus and U.W. Gedde, Nat. Nanotechnol. 5 (2010) p.584.
[82] M. Wang, I.V. Anoshkin, A.G. Nasibulin, J.T. Korhonen, J. Seitsonen, J. Pere, E.I. Kauppinen, R.H.A. Ras and O. Ikkala, Adv. Mater. 25 (2013) p.2428.
[83] S. Volz, Int. J. Heat Mass Transf. 49 (2006) p.251.
[84] W. Wang and W. Liu, J. Beijing Univ. Chem. Technol. Nat. Sci. 37 (2010) p.16.
[85] J. Zhou and J. Balandin, J. Appl. Phys. 89 (2001) p.2933.
[86] S.Q. Zeng and A. Hunt, J. Heat Transf. 117 (1995) p.758−762.
[87] S. Yang and W. Tao, *Heat Transfer Theory*. China Higher Education Press (CHEP), Beijing, 1998.
[88] R.W. Pekala, J. Mater. Sci. 24 (1989) p.3221.
[89] http://www.eyoungindustry.com/uploadfile/file/20151026/20151026224815_41334.pdf
[90] M. Wiener, G. Reichenauer, S. Braxmeier, F. Hemberger, and H.P. Ebert, Int. J. Thermophys. 30 (2009) p.1372.
[91] L.W. Hrubesh and R.W. Pekala, J. Mater. Res. 9 (1994) p.731.
[92] W.C. Li and M. Reichenauer, Carbon 40 (2002) p.2955.
[93] R. Petricevic, M. Glora and J. Fricke, Carbon 39 (2001) p.857.
[94] Y.J.J. Lee, J.C. Jung, J. Yi, S.-H. Baeck, J.R. Yoon and I.K. Song, Curr. Appl. Phys. 10 (2010) p.682.
[95] R.W. Pekala, J. Mater. Sci. 24 (9) (1989) p.3221.
[96] R.W. Pekala and F.M. Kong, J. de Phys. 50 (C4) (1989) p.C433.
[97] M.R. Wiener, G. Reichenauer, F. Hemberger and H.P. Ebert, Int. J. Thermophys. 27 (2006) p.1826.
[98] D. Klemm, F. Kramer, S. Moritz, T. Lindstrom, M. Ankerfors, D. Gray, and A. Dorris, Angew. Chem. Int. Ed. 50 (2011) p.5438; Angew. Chem. Int. Ed. 123 (2011) p.5550.
[99] M. Hamedi, E. Karabulut, A. Marais, A. Herland, G. Nystrçm and L. Wgberg, Angew. Chem. Int. Ed. 52 (2013) p.12038; Angew. Chem. Int. Ed. 125 (1998) p.12260. .
[100] M. Paakko, J. Vapaavuori, R. Silvennoinen, H. Kosonen, M. Ankerfors, T. Lindstrçm, L.A. Berglund and O. Ikkala, Soft Matter 4 (2008) p.2492.
[101] H. Sehaqui, Q. Zhou and L.A. Berglund, Compos. Sci. Technol. 71 (2011) p.1593.
[102] W. Chen, Q. Li, Y. Wang, X. Yi, J. Zeng, H. Yu, Y. Liu and J. Li, Chem. Sus. Chem. 7 (2014) p.154.
[103] L. Heath and W. Thielemans, Green Chem. 12 (2010) p.1448.
[104] I. Sakurada, Y. Nukushina and T. Ito, J. Polym. Sci. 57 (1962) p.651.
[105] J. Wohlert, M. Bergenstrhle-Wohlert and L.A. Berglund, Cellulose. 19 (2012) p.1821.
[106] T. Saito, R. Kuramae, J. Wohlert, L.A. Berglund and A. Isogai, Biomacromolecules 14 (2013) p.248.
[107] M. Paakko, J. Vapaavuori, R. Silvennoinen, H. Kosonen, M. Ankerfors, T. Lindstrçm, L.A. Berglund, and O. Ikkala, Soft Matter 4 (2008) p.2492.
[108] A.J. Svagan, M.A.S.A. Samir and L.A. Berglund, Adv. Mater. 20 (2008) p.1263.
[109] J. Cai, S. Liu, J. Feng, S. Kimura, M. Wada, S. Kuga and L. Zhang, Angew. Chem. Int. Ed. 51 (2012) p.2076; Angew. Chem. Ed. Int. 124 (2012) p.2118.
[110] http://aerotherminsulation.com/sites/default/files/Aero therm%20Tech%20Datasheet%202012.pdf
[111] F. Liebner, E. Haimer, A. Potthast, D. Loidl, S. Tschegg, M.A. Neouze, M. Wendland and T. Rosenau, Holzforschung 63 (2009) p.3; 63 (3) (2009).
[112] http://www.aerotherminsulation.com/products-applications/universal-components-footwear
[113] M.J. Augustyniak and T.D. McCoy, U.S. Patent No. 8,899,000, December 2, 2014, Birdair, Inc.
[114] R.A. Haefer, *Cryopumping, Theory and Practice*, Clarendon Press, Oxford, 1989, p.54.
[115] http://www.birdair.com/tensile-architecture/membrane/insulated-tensioned-membrane
[116] Y. Alison, www.ydalison.com/EN/.

[117] http://www.thermablok.co.uk/wp/wp-content/uploads/2015/11/thermablokaerogelblanketdatasheet2.pdf
[118] K.I. Jensen, J. Non-Crystalline Solids 145 (1992) p.237.
[119] R. Baetens, B.P. Jelle, and A. Gustavsen, Energy Buildings 43 (4) (2011) p.761.
[120] J.E. Fesmire, S.D. Augustynowicz, and S. Rouanet, *Aerogel beads as cryogenic thermal insulation system*, in *Proceedings of the Cryogenic Engineering Conference (CEC '01)*, vol. 613 of *Advances in Cryogenic Engineering*, Madison, WI, July 2001, p.1541−1548.
[121] A.L. Nayak and C.L. Tien, Adv. Cryogenic Eng. 22 (1977) p.251.
[122] R. Wawryk and J. Rafalowicz, Int. J. Thermophys. 9 (4) (1988) p.611.
[123] M.J. Burchell, M.J. Cole, M.C. Price and A.T. Kearsley, Meteoritics Planetary Sci. 47 (4) (2012) p.671.
[124] J.E. Fesmire, Cryogenics 46 (2−3) (2006) p.111.
[125] M. Tabata, I. Adachi, Y. Ishii, H. Kawai, T. Sumiyoshi and H. Yokogawa, Nucl. Inst. Methods Phys. Res. A 623 (1) (2010) p.339.
[126] N.J.H. Dunna, M.K. Carrolla and A.M. Anderson, Polym. Preprints 52 (1) (2011) p.250.
[127] R. Yang, Y.P. Zhang and R.Y. Zhao, J. Air Waste Manag. Assoc. 54 (12) (2004) p.1516.
[128] K. Kanamori, J. Ceramic Soc. Japan 119 (1385) (2011) p.16.
[129] J.L. Plawsky, H. Littman and J.D. Paccione, Powder Technol. 199 (2) (2010) p.131.
[130] H. Ramadan, T. Coradin, S. Masse, and H. El-Rassy, Silicon 3 (2) (2011) p.63.
[131] N. Leventis, Acc. Chem. Res. 40 (9) (2007) p.874.
[132] D.J. Boday, P.Y. Keng, B. Muriithi, J. Pyun and D.A. Loy, J. Mater. Chem. 2 (33) (2010) p.6863.
[133] J. Fricke and A. Emmerling, J. Sol-Gel Sci. Technol. 13 (1−3) (1999) p.299.
[134] Y. Guo and A.R. Guadalupe, Chem. Commun. (4) (1999) p.315.
[135] S. Dai, Y.H. Ju, H.J. Gao, J.S. Lin, S.J. Pennycook and C.E. Barnes, Chem. Commun. (3) (2000) p.243.
[136] N. Leventis, C. Sotiriou-Leventis, G. Zhang and A.M.M. Rawashdeh, Nano Lett. 2 (9) (2002) p.957.
[137] *Cryogel 5201*, 10201 Safety Data Sheet, Aspen Aerogel. 11/13/07. Available at http://www.oalib.com/references/13872765
[138] N. Terry, J. Palmer, and I. Cooper, *DCLG State-of-the-Art Review: Insulation and Thermal Storage Materials*. DCLG, London, 2012. Available at http://www.carltd.com/sites/carwebsite/files/Insulation%20and%20thermal%20storage%20materials%20pre-publication%20draft_1.pdf
[139] Cabot Corp. Available at http://wl.cabot-coro.comlcontroller.jsp?N=23+4294967102+3153&entry=product.
[140] I. Aspen Aerogel. Available at *http://www.aerogel.comlproducts.htm*.
[141] http://www.maerotech.com/prospect3.html
[142] http://www.cabotcorp.com/solutions/products-plus/aerogel/
[143] http://www.aerogel.com/.
[144] http://www.chem-eng.kyushu-u.ac.jp/e/research.html..
[145] L.L. Jianjun Shi, W. Guo, J. Zhang and Y. Cao, Carbohydrate Polym. 98 (2013) p.282.
[146] T.S. Yuri Kobayashi and A. Isogai, Angew. Chem. Int. Ed. Engl. 53 (39) (2014) p.10394.
[147] ASPEN. Available at www.aerogel.com
[148] H. Sehaqui, M. Salajkov, Q. Zhou and L.A. Berglund, Soft. Matter 6 (2010) p.1824.
[149] http://www.innovationintextiles.com/industry-talk/aerotherm-aerogel-insulation-brings-space-technology-to-everyday-life/.
[150] E. Cuce, P. Mert Cuce, C.J. Wood and S.B. Riffat, Renew. Sust. Energy Rev. 34 (2014) p.273.